THE UNIVERSITY OF QUEENSLAND

AUSTRALIA

Efficacy of a novel neuronal death inhibitor in Alzheimer's disease models

Aanchal Sharma

BsC Honours

A thesis submitted for the degree of Master of Philosophy at

The University of Queensland in 2014

Queensland Brain Institute

Abstract

Alzheimer's disease is the most common cause of dementia affecting 5% of the population between 65-74 years and 50% over 80 years. Despite its increasing burden, there are currently no treatments available to stop or slow down the degeneration associated with AD. The therapies that are available merely alleviate the symptoms with minimal impact on disease progression.

Neurotrophin dysfunction has been implicated in AD including the activation of the p75 neurotrophin receptor (p75NTR) mediated neuronal death signalling. Our lab has been investigating the p75NTR cell death pathway for a number of years and has characterised a 29 amino acid intracellular juxtamembrane domain of p75NTR that is capable of preventing p75NTR mediated cell death *in vitro.* Due to the involvement of p75NTR death signalling in neurodegenerative diseases such as AD, any compound that inhibits the activation of p75NTR cell death signalling can be therapeutically beneficial.

The goal of my research was to test the efficacy of this 29 amino acid domain peptide (biotin-TAT-c29) *in vivo*. In order to examine this, firstly we had to develop/characterize an animal model of degeneration. This study characterized three different models: i) SAMP8 model of basal forebrain death, ii) neurotrophin dependent model of basal forebrain death and iii) Aβ mediated hippocampal toxicity model. Secondly, the protocol for the delivery of the peptide into the brain was optimized through both intraperitoneal injection and subcutaneous osmotic pumps. Finally, the ability of the biotin-TAT-c29 peptide to prevent degeneration was tested. We successfully characterised two possible models of degeneration to test the efficacy of the biotin-TAT-c29 peptide. We also established a robust protocol for the delivery and detection of the biotin-TAT-c29 peptide into the central nervous system. While the results from the final experiment involving the delivery of biotin-TAT-c29 into a degeneration model were equivocal, other work from the lab indicates the promising therapeutic nature of this peptide suggesting that further studies should be pursued using biotin-TAT-c29.

Declaration

This thesis *is composed of my original work, and contains* no material previously published or written by another person except where due reference has been made in the text. I have clearly stated the contribution by others to jointly-authored works that I have included in my thesis.

I have clearly stated the contribution of others to my thesis as a whole, including statistical assistance, survey design, data analysis, significant technical procedures, professional editorial advice, and any other original research work used or reported in my thesis. The content of my thesis is the result of work I have carried out since the commencement of my research higher degree candidature and does not include a substantial part of work that has been submitted *to qualify for the award of any* other degree or diploma in any university or other tertiary institution. I have clearly stated which parts of my thesis, if any, have been submitted to qualify for another award.

I acknowledge that an electronic copy of my thesis must be lodged with the University Library and, subject to the General Award Rules of The University of Queensland, immediately made available for research and study in accordance with the *Copyright Act 1968*.

I acknowledge that copyright of all material contained in my thesis resides with the copyright holder(s) of that material. Where appropriate I have obtained copyright permission from the copyright holder to reproduce material in this thesis.

Publication during candidature

An intracellular domain fragment of the p75 neurotrophin receptor enhances TrkA receptor function

Dusan Matusica, Sune Skeldal, Alex M. Sykes, Nickless Palstra**, Aanchal Sharma** and Elizabeth J.Coulson

Published in The Journal of Biochemistry (2013)

Publications included in this thesis

Publication citation – incorporated in Chapter 1 background work performed during summer studentship. The experiment included was performed 100% by me and designed by the author of the publication and supervisor (Dusan Matusica and Elizabeth Coulson)

An intracellular domain fragment of the p75 neurotrophin receptor enhances TrkA receptor function

Dusan Matusica, Sune Skeldal, Alex M. Sykes, Nickless Palstra**, Aanchal Sharma** and Elizabeth J.Coulson

Published in The Journal of Biological Chemistry (2013)

Contributions by others to the thesis

No significant contribution by others.

Statement of parts of the thesis submitted to qualify for the award of another degree

None

Acknowledgements

First and foremost I would like to thank my supervisor Associate Professor Elizabeth Coulson. Lizzie, thank you for giving me this opportunity to work with you. Your optimistic attitude, commitment and passion towards research have been such an inspiration. Your enthusiasm never failed to motivate me and I am grateful for all the guidance I have received from you over the years.

Secondly, I would like to thank my two co-supervisors: Dr. Fabienne Alfonsi and Dr. Dusan Matusica. Fabienne, in simple words “I am not sure what I would have done without you!”. Thank you for being so patient with me, thank you for directing me every step of the way, thank you for not only being a brilliant supervisor but also being a friend. I can’t thank you enough, all I can say is Fab you are fab! Next I would like to thank Dusan. Dusan, I have appreciated all the help and guidance I have received from you. Thank you for your support and advice along the way, I have learnt so much from you.

I would now like to thank the most amazing (past and present) members of the Coulson Lab: Toni, Nick, Zoran, Linda, Sune and Georg. You guys made my time in the lab absolutely wonderful. Thanks for brightening up my day with all the fun conversations, the laughs, the never ending hilarious jokes and most of all thank you for making me realize that working in a lab doesn’t have to be all serious and boring. A very very special thank you to Toni for always being there through thick and thin. You and your friendship means so much to me. I wouldn’t have gotten through this without our numerous (and lengthy) coffee and lunch breaks! I have found a life long friend in you.

I would also like to thank my wonderful partner Chetan for being there for me throughout this whole journey. Thank you for sharing my joy during the happy times and holding my hand and motivating me through the tough ones. Thank you for all your understanding and support through this bumpy ride! Last but not the least a big thanks to my family for all your love and encouragement. Love you guys.

Keywords

Neurotrophins, p75NTR, Alzheimer's disease, Amyloid Beta, APP models, Saporin

Australian and New Zealand Standard Research Classifications (ANZSRC)

060110 Receptors and Membrane Biology 60%

060111 Signal Transduction 20%

110902 Cellular Nervous System 20%

Fields of Research (FoR) Classification

1109 Neurosciences 30%

0601 Biochemistry and Cell Biology 70%

Table of Contents

List of Figures

List of Abbreviations

AD	Alzheimer's disease
APP	Amyloid precursor protein
Aβ	Amyloid beta
c29	Juxtamembrane 29 amino acid domain
cBF	Cholinergic basal forebrain
cBFN	Cholinergic basal forebrain neurons
ChAT	Choline O-acetyltransferase
CTF	C-terminal fragment
ECD	Extracellular domain
HDB	Horizontal diagonal band
ICD	Intracellular domain
ICV	Intracerebroventricular
LDT	Laterodorsal tegmentum
MPT	Mesopontine tegmentum
MS	Medial Septum
NGF	Nerve growth factor
p75NTR	p75 neurotrophin receptor
PPT	Pendunculopontine tegmentum
PTD	Protein transduction domain
REM	Rapid Eye Movement
SAMP8	Senescence accelerated mouse (strain 8)
SAP	Saporin
TAT	Trans-activating transcriptional activator
TrkA	Tyrosine kinase A
VDB	Vertical Diagonal Band

Chapter 1 - Introduction

1.1. Alzheimer's disease

Alzheimer's disease (AD) accounts for about 60-70% of all dementia cases and results in memory loss and decline in cognitive abilities (Holtzman et al., 2011). Key hallmarks of AD include amyloid beta (Aβ) plaques, neurofibrillary tangles and extensive neuronal loss (Holtzman et al., 2011). There are three main hypotheses to explain the cause of the disease: the amyloid hypothesis, the tau hypothesis and the cholinergic hypothesis.

The *Amyloid Hypothesis* of AD proposes that the accumulation and aggregation of Aβ within the brain is the primary cause of cognitive decline and degeneration seen in AD (Glenner and Wong, 1984, Masters et al., 1985, Hardy and Selkoe, 2002, Tanzi, 2005). Aβ is the product of beta (β) and gamma (γ) secretase cleavage of the amyloid precursor protein (APP). Most evidence for this hypothesis is based on familial cases of AD due to mutations in three key genes the Aβ precursor protein (APP) itself, Presenilin 1 and 2, the enzymatic component of γ-secretase (Hardy et al, 1995). These mutations result in overproduction of Aβ by enhancing the processing of APP to Aβ or by generating forms of Aβ that are particularly prone to aggregation and thus are neurotoxic (Hardy et al., 1998, Tanzi and Bertram, 2005). The Aβ42 isoform (that is 42 amino acids long) of Aβ is more prone to aggregation than the Aβ40 isoform, which gives rise to toxic dimers, oligomers and fibrils and ultimately to the production of plaques.

The *Tau Hypothesis* of AD argues that neurofibrillary tangles are the primary cause of AD (Lee et al., 2001b). The tangles are comprised of microtubule-associated protein called Tau which is normally expressed in axons. During AD, Tau protein becomes hyperphosphorylated and aggregates into abnormal fibrillary filaments in the cell body resulting in microtubule disintegration and collapse of the neuronal transport system eventually leading to neuronal death (Mudher and Lovestone, 2002, Iqbal et al., 2005, Chun and Johnson, 2007). However, no mutations have been reported in the Tau gene that result in AD. Rather, more recent evidence has suggested Tau pathology to be downstream of Aβ pathophysiology (Ittner and Gotz, 2011). Taken together with the strong support for the amyloid hypothesis in mouse models where overproduction of Aβ results in cognitive deficits, the findings argue Aβ to be the proximal cause of AD as opposed to Tau.

However, phosphorylated-tau could be acting together with Aβ to mediate neuro-toxicity (Gotz et al., 2011, Ittner and Gotz, 2011).

The *Cholinergic Hypothesis* proposes that cognitive decline seen in AD is in response to the degeneration of cholinergic basal forebrain (cBF) neurons (Bartus et al., 1982). The cholinergic basal forebrain refers to the area of the brain derived from the subpallium and located close to the medial and ventral surfaces of the cerebral hemisphere. It comprises of different nuclei including the medial septum (MS), vertical and horizontal diagonal bands (VDB and HDB) nucleus basalis and substantia innominata. The release of acetylcholine from innervating cBF neurons normally regulates the excitability and plasticity of neocortical areas, which in turn controls higher order cognitive functions such as attention, learning and memory (Coyle et al., 1983, Sarter and Bruno, 2004). Therefore, the degeneration of cBF neurons results in the loss of this cholinergic neurotransmission in the cerebral cortex, hippocampus and other areas that play a significant role in learning and memory (Bartus et al., 1982, Terry and Buccafusco, 2003). In AD, 75% of cBF neurons are selectively lost coincident with frank loss of presynaptic cholinergic markers throughout the cortex (Whitehouse, 1991a, b). The hypothesis that loss of acetylecholine to the cortex underpins the cognitive decline seen in AD served as the basis for the main therapeutic approaches that currently exist for AD.

The cholinergic basal forebrain neurons are highly dependent on neurotrophin survival signalling throughout life. Nerve growth factor (NGF) is the principal target derived neurotropic factor that not only protects cBF neurons from insults and age dependent atrophy but also potentially regulates their phenotype and plasticity (Brooks et al., 2000a). TrkA receptor for NGF mediates signal transduction pathways important for promoting and maintaining synaptic contact with cortical and hippocampal neurons and for cBF neuron survival. An imbalance in this signalling due to reduced levels of NGF and/or TrkA observed in AD subjects at post-mortem, can impact memory formation and neuronal degeneration (Mufson et al., 1997, Capsoni et al., 2000). This forms the basis for the *neurotrophic hypothesis* which states that a dysfunction of neurotrophin survival signalling is responsible for the degeneration of cholinergic neurons in Alzheimer's disease.

1.2. Neurotrophins in AD

Neurotrophins are a family of growth factors that play important roles in both the developing and adult brain to regulate neuronal survival and death. Four neurotrophins that exist in a mammalian brain include NGF, brain-derived neurotrophic factor (BDNF), neurotrophin-3 (NT-3) and neurotrophin-4 (NT-4) (Dechant and Barde, 2002, Underwood and Coulson, 2008, Skeldal et al., 2011). Neurotrophins exhibit their vast range of functions via two structurally different receptors: the tropomyosin receptor-like kinase (Trk) receptors and the p75 neurotrophin receptor (p75NTR) (Hennigan et al., 2007). While the signalling pathways activated by the Trk receptor family are well characterized in the literature as predominantly trophic, p75NTR can mediate a range of signalling outcomes.

Originally, p75NTR was known to act as a co-operative facilitator of the Trk receptors by forming a high affinity NGF receptor complex (Hempstead et al., 1991). This results in activation of survival signalling to allow cell proliferation, migration, neurite elongation/retraction and synaptic transmission in response to minimal amounts of NGF available *in vivo* (Davies, 1991, Barker, 2004). However, later it was demonstrated that the receptor could signal cell death in the absence of appropriate Trk activation (Coulson et al., 2000b, Dechant and Barde, 2002, Coulson et al., 2009). Pro-neurotrophins are the precursor form of the mature neurotrophins and have been exclusively shown to promote cell death via the p75NTR both in the presence and absence of Trk receptors (Skeldal et al., 2011).

In the developing nervous system, p75NTR is widely expressed in the central nervous system where it regulates synaptogenesis and developmental cell death (Davies, 1991). The expression of p75NTR is down regulated post development in most brain regions. However, some pathological conditions like mechanical damage, focal ischemia, epilepsy, axotomy and neurodegenerative disorders such as AD can result in re-expression of p75NTR at levels comparable to that during development, and can signal neuronal death (Lowry et al., 2001).

Interestingly, the cBF neurons continue expressing p75NTR throughout adult life. cBF neurons project their axons to the hippocampus and cortex which produce the survival-promoting on which cBF neurons are dependent on for survival (Coulson et al., 2000b, Ginsberg et al., 2006). The role of p75NTR in cBF neurons may either be: strengthening cBF neuron innervations (to their target neurons by facilitating Trk mediated trophic

signalling) or pruning neurons that do not receive sufficient trophic support (Naumann et al., 2002). Enhancing NGF expression in the cBF either exogenously or via repetitive learning tasks results in an augmentation of synaptic function and memory due to an increase in cBF neuron innervations to the cortex (Brooks et al., 2000a, Brooks et al., 2000b, Prakash et al., 2004). In contrast, a reduction in NGF supplied to the cBF lowers the density of cBF neuron innervations to their targets therefore reducing synaptic plasticity (Gutierrez et al., 1997). These changes associated with varying NGF levels signify the importance of TrkA and p75 signalling in the maintenance of cBF.

Cognitive changes occurring in AD could be due to the dysfunction of the neurotrophin signalling in the basal forebrain, as decreased levels of NGF and TrkA have been reported in AD patients (Mufson et al., 1992, Fahnestock et al., 2001, Ginsberg et al., 2006). Furthermore, in AD the levels of cell death-inducing pro-neurotrophins and p75NTR are up-regulated, shifting the balance of neurotrophin survival signalling to death signalling and resulting in reduced cBF neuron number and subsequently facilitating degeneration of the denervated cortical and hippocampal neurons (Nagappan and Lu, 2005).

In animal models of neurodegeneration, including AD, blocking p75NTR signalling has been shown to prevent cell death, highlighting the importance of p75NTR as a candidate therapeutic target (Sotthibundhu et al., 2008, Yang et al., 2008, Knowles et al., 2009). Being able to interfere with the ability of p75NTR to signal neuronal death, or enhancing p75NTR-facilitated Trk survival signalling may be highly beneficial in promoting neuron survival in a number of p75NTR-mediated neurodegenerative disorders.

1.3. A juxtamembrane domain peptide of p75NTR as a neuroprotectant

1.3.1 Regulation of p75 survival and death signalling functions

The opposing survival and death functions of p75NTR described above can be partially explained by the receptor's ability to undergo regulated proteolysis. p75NTR can signal constitutively in the unbound and monomeric state as a result of regulated intramembrane proteolysis whereby the extracellular domain (p75NTR-ECD) is cleaved by an α-secretase (ADAM17/TACE). This results in a membrane tethered C-terminal fragment (CTF), which undergoes subsequent cleavage by the presenilin-dependent γ-secretase releasing the intracellular domain (p75NTR-ICD) fragment into the cytoplasm (Lee et al., 2001a, Jung et al., 2003, Kanning et al., 2003).

It has previously been shown by the Coulson laboratory that the membrane bound p75NTR-CTF induces cell death whereas the p75NTR-ICD fragment, free in the cytosol facilitates survival signalling (Coulson et al., 1999, Coulson et al., 2000a, Underwood et al., 2008). Our lab has also found that the p75NTR-ICD can promote survival signalling through interacting with Trk receptors (Ceni et al., 2010, Kommaddi et al., 2011, Matusica et al., 2013). Others have also reported that the p75ICD fragment can promote survival signalling (Ceni et al., 2010, Kommaddi et al., 2011) as well as, neurite outgrowth, differentiation and cell death (Frade, 2005; Kenchappa et al., 2006; Bronfman, 2007; Skeldal et al., 2011). These findings suggest that the cleavage of p75NTR ectodomain is necessary for the physiological activation of p75NTR (Skeldal et al, 2011).

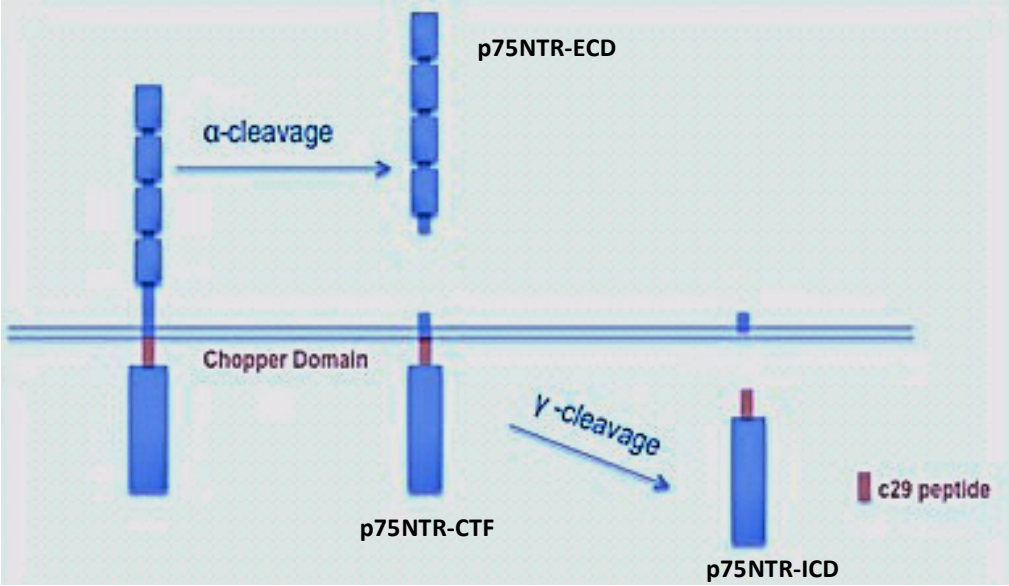

Figure 1.1- Schematic of p75NTR cleavage

The full-length p75NTR undergoes intramembranous proteolysis mediated initially by the α -secretase releasing the ECD fragment. The C-terminal fragment (CTF) attached to the membrane has been shown to promote cell death even in the absence of ligand. A γ-secretase subsequently cleaves CTF, liberating an intracellular domain fragment (ICD). c29 (indicated in red) is the 29 amino acid fragment of the juxtamembrane domain.

A key discovery underpinning the Coulson lab discovery of opposing roles for the p75NTR fragments was the identification and characterisation of the Chopper domain of p75NTR (Coulson et al., 1999, Coulson et al., 2000a). This juxtamembrane domain comprises a 29 amino acid sequence (KRWNSCKQNKQGANSRPVNQTPPPEGEKLHSDSGI). When tethered to the membrane this peptide (c29) promotes cell death, however when unattached to the cell membrane the peptide inhibits cell death (Coulson et al., 2000a, Matusica et al., 2013). The ability of c29 to inhibit neural death suggested a dominant-

negative mechanism whereby both the membrane bound and unbound forms were interacting with the same accessory proteins. p75NTR-CTF when free in the cytosol may also be able to sequester these proteins and inhibit their action thereby contributing to the dominant negative signalling of p75NTR (Coulson et al., 2000a, Coulson et al., 2004).

However, recent work from the lab that aimed to understand the exact mechanism by which c29 mediates its action revealed the ability of c29 to interact with TrkA and TrkB receptors. The experiment, to which I contributed, involved immunoprecipitation of the Trk receptors with a biotinylated c29 peptide. The immunoprecipitated complex was then detected using the receptor specific antibodies. While both TrkA and TrkB could be immunoprecipitated, the epidermal growth factor (EGF) receptor, a tyrosine kinase receptor with homology to the Trk receptors, did not associate with c29 (Matusica et al, 2013).

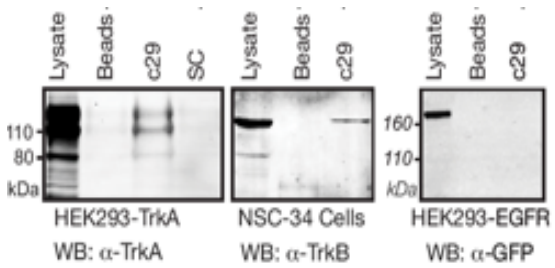

Figure 1.2 - c29 interacts with Trk A and Trk B but not EGFR receptor

The western blot shows an immuneprecipitation experiment. Biotinylated c29 peptide was used to precipitate TrkA, TrkB and EGFR from cell lysates. The figure shows that c29 can immunoprecipitate with Trk A (HEK293 cells transfected with the TrkA receptor) and Trk B (NSC34 cells that endogenously expressing the Trk B receptor). There was no interactions seen with scrambled c29 and c29 does not immunoprecipitate with the EGFR receptor (Matusica et al., 2013).

The c29 peptide also enhances NGF binding to TrkA receptor resulting in a 3-fold increase in receptor association rate as well as an increase in the number of receptor sites capable of binding NGF (Matusica et al., 2013). It is therefore postulated that c29 could be acting as an allosteric modulator of the Trk receptors and potentiating neurotrophic signalling by creating high affinity neurotrophin binding sites to promote survival signalling instead, or as a dominant negative inhibitor of death signalling (Matusica et al., 2013). Either function would make c29 a therapeutic agent to block p75NTR mediated cell death in neurodegenerative diseases like AD where neurotrophin signalling is compromised.

1.3.2 Neuronal protection by c29

Study of the c29 peptide has been a focus of Coulson and colleagues for many years. It has been demonstrated that c29 inhibits $p75^{NTR}$-mediated death signals during naturally-occurring developmental cell death in the chick eye (Coulson et al., 2000a), protects sensory and motor neurons from growth-factor withdrawal-induced cell death *in vitro* and injury- and amyotrophic lateral sclerosis -like disease-induced cell death of motor neurons *in vitro* and *in vivo* (Matusica et al., submitted). One example of its effect *in vivo* is an axotomy experiment. After axotomy 50% of cervical motor neurons of new-born rats die because they no longer receive BDNF from their target muscle. When a c29-peptide was placed at the axonal stump of the rat pups, it protected motor neurons, as assessed 5 days later (~10% cell death compared to ~50% $p<0.01$). These experiments suggest the c29 peptide has both a novel therapeutic property and *in vivo* efficacy to promote neuronal survival in conditions of neurotrophin signalling imbalance.

Altered neurotrophin signalling in AD is not only caused by an altered expression of the neurotrophins and their receptors but also by the presence of Aβ. Aβ is known to be a ligand for p75NTR providing a possible mechanism via which Aβ toxicity in AD may be mediated (Yaar et al., 1997, Coulson et al., 2008, Sotthibundhu et al., 2008, Yang et al., 2008, Knowles et al., 2009). The Coulson colleagues have additionally shown that Aβ can inhibit γ-secretase cleavage of the p75NTR, thereby promoting cell death through p75NTR-CTF and preventing participation of p75NTR-ICD in Trk mediated survival signalling (Sotthibundhu et al., 2008). Moreover, a former PhD student (Linda May, Manuscript submitted, 2014) found that the addition of c29 peptide to E16.5 hippocampal cultures blocked the toxic effects of Aβ42 (Fig 1.3).

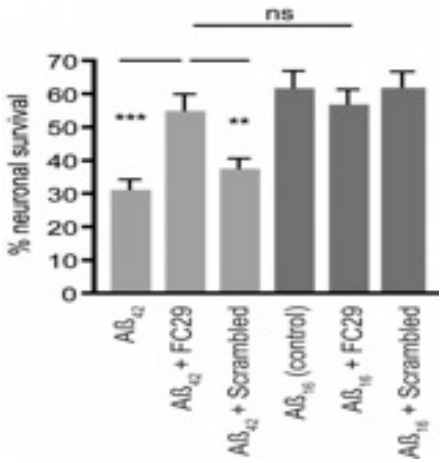

Figure 1.3 - c29 blocks Aβ mediated death in hippocampal neurons

E18 hippocampal cultures were grown in the presence of Aβ and c29. Cell counts were performed to determine rates of survival over the 24 hours. Addition of Aβ42 to primary hippocampal neuron culture results in the survival of only 30% of cells. When c29 is added together with Aβ42, the survival of these neurons was significantly increased to 55%, a survival rate not significantly different from control-treated cultured ~60%) This protective effect is not seen with the scrambled control peptide (May et al, 2013 – manuscript submitted).

In summary, the neurotrophins can influence the survival signalling of cBFNs as well as impact the production of toxic Aβ. The evidence for the neuroprotective ability of c29 peptide has been shown both in the context of growth factor withdrawal and in conditions of neurotroxic Aβ42. As reduced supplies of neurotrophins and Aβ toxicity are two key pathophysiological features of AD the aim of this project was to test the efficacy of c29 peptide in *in vivo* models of Alzheimer's disease.

1.4. Existing mouse models of Alzheimer's disease

In order to better understand the pathophysiology of AD a number of experimental animal models have been established. Mouse models based on genetically manipulating particular gene function and expression allow us to study the function and affects of the resulting proteins and their involvement in disease conditions. In addition, the use of mice allow behavioural studies for examination of cognitive abilities (e.g. the clinical phenotype of AD) and are the predominant preclinical organism for screening of candidate drugs.

The most widely used mouse models of AD are based on the transgenic expression of human APP cDNA (hAPP). A number of transgenic hAPP mouse lines exist, for example: i) PDAPP mice expresses hAPP 770 isoform with Indiana mutation (V717F), which

exhibits Aβ plaque pathology at 2 years of age and a decrease in synaptic and dendritic density in the hippocampus without any neuron loss (German et al., 2003) ii) the Tg2576 mouse model is generated by the overexpression of hAPP695 construct that contains a double Swedish mutation (K670N/M671L). These mice express 5-6 times more hAPP, exhibit plaque deposition at 9-12months of age, but again show no neuron loss (Sturchler-Pierrat et al., 1997). iii) APP23 mice express APP Swedish mutation under the control of Thy1 promoter and show a decrease in cholinergic fibre density at 24 months of age but no loss of cBF neurons (Boncristiano et al., 2002). In general the hAPP transgenic models exhibit synaptotoxicity but fail to show any neuron loss.

Presenilin mutations have also been used to develop AD mouse models. However, it was noted that a single presenilin mutation in mice did not result in AD like pathology due to differences between the mouse and human APP/Aβ (Selkoe, 1989, Holcomb et al., 1999). Combination of the presenilin mutation with hAPP mutation however results in accelerated AD pathology with mice exhibiting extensive plaque pathology and behavioural deficits (Duff et al., 1996, Jankowsky et al., 2004). The most commonly used line combines transgenes expressing hAPP with the Swedish mutation and presenilin 1 containing a ΔE9 mutation. These mice develop amyloid plaques and cognitive deficits at 6-7 months of age (Jankowsky et al., 2004). While dystrophic cholinergic neurites with a significant reduction in cholinergic fibres in the cortex and hippocampus can be seen, these mice also do not exhibit any significant neuron loss (Perez et al., 2007).

Many transgenic APP models of AD are reliably able to replicate the Aβ pathology seen in human condition but fail to recapitulate tau pathology. Similarly, most tau transgenic mice do not exhibit Aβ pathology. Therefore, most tau mutation models of AD are in conjunction with the hAPP models, as tau mutations alone do not cause AD (Oddo et al., 2003). A well-characterised model of AD incorporating tau mutations and Aβ overproduction is the 3xTg model of AD which combines mutant hAPP, PS1 and tau transgene. Mice of this strain develop plaques and subsequent neurofibrillary tangles as seen in human AD (Oddo et al., 2003).

While all the models described above have been useful for the particular purpose for which they were created, none of the models encompass all the pathology and cognitive deficits seen in human AD. Primarily, there is a lack of robust cholinergic cell loss in the basal forebrain suggesting that the current familial models of AD do not replicate the sporadic

disease pathology in terms of neuron loss (Perez et al., 2005). Therefore in order to test the therapeutic potential of c29 peptide in an Alzheimer's disease model, an animal model that encompasses basal forebrain loss and Aβ toxicity first needed to be developed.

Hypothesis and Aims

We hypothesise that the intracellular domain peptide of p75NTR (c29) will prevent neuronal degeneration and cognitive changes in animal models of Alzheimer's disease

Aim 1: to develop a model of neuronal degeneration in mice where the efficacy of c29 in preventing the degeneration can be tested. Three possible models would be investigated:

(i) *Senescence accelerated model of cBF degeneration* – Characterizing this mouse model for basal forebrain death

(ii) *Neurotrophin withdrawal model of cBF degeneration* - Develop a model of neurotrophin dependent basal forebrain death by ablating the laterodorsal tegmental (LDT) neurons using the Urotensin-II saporin toxin

(iii) *Aβ hippocampal degeneration model* – Develop a model of Aβ induced hippocampal degeneration by killing cBF with p75NTR-saporin toxin in double transgenic APP/PS1 mice

Aim 2: to optimize a protocol for systemic delivery and detection of c29 *in vivo*

Aim 3: to investigate the efficacy of c29 peptide in preventing neuronal degeneration in one or more of the mouse models developed in aim 1.

Chapter 2 - Methods

2.1. Animals

All mice were housed in QBI animal facility under standard conditions with 12-hour light/dark cycle, controlled temperatures and humidity, food and water *ad libitum* with bedding and tissues for nesting. All animal experiments were carried out with the approval of the University of Queensland Animal Ethics Committee, which abides by the Australian Code of Practice for the Care and Use of Animals for Scientific Purposes and the *Animal Care and Protection Act (Qld) 2001.* All efforts were made to minimize the number of animals used and their suffering.

2.1.1. C57bl/6j

For all biotin-TAT-c29 delivery optimization experiments (Aim 2), male C57Bl/6J mice between the ages of 10-12 weeks were used. C57bl/6j mice were also used for the neurotrophin withdrawal model of degeneration (Aim 1b). For this model, surgeries were performed on males of age 7-8weeks, weighing between 20-24g.

2.1.2. APP/PS1

APP/PS1 is a double transgenic strain of mice (maintained on c57 background) expressing mutated human amyloid precursor protein (huAPP695swe) and a mutant human presenilin 1 (PS1-dE9) mutation. The mutant human amyloid precursor protein consists of humanized mouse Aβ precursor protein gene which is modified at three amino acids as well as a mutation at K595N/M596L which is linked to familial AD. The PS1 transgene expresses a mutant form of the human presenilin 1 gene with a deletion at exon 9, which is also linked to familial AD. Both mutations result in an early onset of Alzheimer's disease in these mice. The mice were used for surgeries (Aim 1c) age between 2-5months.

2.1.3. SAMP8

The senescence–accelerated prone mouse is an accelerated model of aging which was developed by selective inbreeding of the AKR/J strain of mice. These mice show age-related behavioural deficits in learning and memory, anxiety, impaired immune system, and age dependent Aβ deposition. These mice were used for histological analysis (Aim 1a) from age 3-12 months.

2.2. Peptide synthesis

The juxtamembrane domain of p75NTR ('chopper'), which comprises of 29 amino acids (KRWNSCKQNKQGANSRPVNQTPPPEGEKL) was conjugated to a trans-activating transcriptional activator (TAT) protein transduction domain (PTD: YARAAARNARA) by Auspep Pty. Ltd (Tullamarine, Aus). A control peptide with a randomly scrambled sequence of the c29 peptide (SC: SKGQVCRNQPGQNKPEPANKSWKETPLRN) coupled to PTD was also synthesised. These peptides were labelled at the amino terminus with a biotin tag via a six-carbon spacer to allow detection of the peptides. The peptides were stored at 4^{o}C in powder form and were reconstituted in sterile saline for *in vivo* experiments and MilliQ H_2O for *in vitro* experiments prior to use.

2.3. *In Vivo* systemic administration of c29

All animals weighed between 24g-30g and were randomly assigned into each group. The weight and general health of mice was monitored until sacrifice. Once sacrificed, the delivery of the peptide into the central nervous system was detected either by western blotting or immunohistochemistry of brain and spinal cord tissue.

2.3.1. Intraperitoneal delivery

Mice were injected intraperitoneally with 100µl of biotin-TAT-c29 or control peptide made in sterile saline. For the pilot experiment mice (n=6) were injected with 2mg/kg c29 peptide and were sacrificed at either 1hr, 6hr, 24hr or 72hrs post injection. Mice were also injected at one-day interval for 6 weeks at 2mg/kg, 5mg/kg and 8mg/kg (n=3 per concentration).

2.3.2. Subcutaneous delivery

Peptide delivery was also optimized using subcutaneous osmotic minipumps (Alzet corporation, Palo Alto, CA). For the pilot experiment, two 7-day pumps (Model 1007D with flow rate of 0.5µl/hr) were filled with 100µl of 8mg/kg biotin-TAT-c29 peptide and placed in sterile PBS at 37^{o}C for 3 hours in order to initiate the pump. The mice were then anaesthetised using 5% isofluorane. Once the mouse was anesthetised, the head was cleaned with ethanol and an incision was made over the scalp. A curved haemostat was inserted from this incision in order to break the membranes under the skin and to create a pocket which would hold the pump. Once this pocket was made, the osmotic pump was inserted and placed behind the neck. After surgery, the mouse received a dose of analgesic (Torbugesic,1.3mg/kg) and antibiotic (Baytril, 0.43mg/kg). The mice were

sacrificed one week after the surgery and the results were compared to mice intraperitoneally injected with biotin-TAT-c29.

2.4. In Vitro experiments with c29

2.4.1. ERK activation

PC12 cells were cultured in Dulbecco's modified Eagle's medium (DMEM) supplemented with 10% foetal calf serum (FCS), 5% horse serum and 1% Glutamax. Cells were grown in a humidified 37^{o}C incubator with 5% CO_2 atmosphere. For the ERK activation assay, cells were plated in a 6-well plate poly-L-ornithine (0.015%) coated plates at 0.5 million cells/well and incubated overnight till confluent. Following day, the cells were serum starved in serum free media comprised of DMEM, 1% Glutamax and 1% non-essential amino acids for four hours at 37^{o}C. An hour before lysis, some wells were treated with 1μM of biotin-TAT-c29 peptide and incubated. Ten minutes before lysis, the cells were treated with different concentration of NGF. The following NGF treatment conditions were used: 0ng/ml (control), 1ng/ml, 10ng/ml, 100ng/ml, 1ng/ml + c29 and 10ng/ml + c29. Cells were incubated with NGF for 10 minutes to initiate an ERK response before they were lysed.

2.4.2. Lysis, Immunoprecipitation and Western Blotting

After intraperitoneal injection of the peptide, brain and spinal cord were harvested. Total protein was extracted by lysing the tissue in TNE buffer (20 mm Tris, pH 8, 10 mm EDTA) supplemented with 1% Nonidet P-40 and complete protease inhibitor mixture (Roche Applied Science). The lysates were homogenised in the tissue homogeniser using magnetic beads for 3 minutes. The crude homogenate was centrifuged at 14000x g for 15 minutes at 4^{o}C. The supernatant was removed and spun for another 10 minutes.

To perform protein immunoprecipitations, the lysates were incubated with Dynabeads MyOne Streptavidin T1 (Invitrogen), 2% Bovine Serum Albumin (BSA) and PBS overnight at 4^{o}C to allow interactions between the biotinylated peptide and streptavidin. The immunocomplexes were then thoroughly washed (5 times) with Tris Buffered Saline (TBS; 10 mM Tris pH 8.0, 150 mM NaCl) supplemented with 0.05% Tween 20 to prevent non-specific binding. The samples were eluted in reducing sample buffer (20mM Dithiothreitol, 2.5% SDS). For western blotting the samples were boiled at 95^{o}C for 5 minutes and then subjected to reducing conditions on 12% SDS-PAGE gels (Invitrogen) for 90 minutes at 130V. The proteins were transferred onto a nitrocellulose membrane at 90V for 90

minutes. The membrane was blocked in TBS-Tween (TBST; 10 mM Tris, pH 8.0; 150 mM NaCl; and 2% Tween 20) supplemented with 5% (w/v) dried skim milk powder for 1 hour at room temperature. The membrane was probed for biotin-TAT-c29 peptide with primary rabbit anti-human p75NTR intracellular antibody (9992: used at concentration 1:1000, binding resides 276-399 (Huber & Chao, 1995)) overnight at 4^{o}C or 3 hours at room temperature. This was followed by 3 times 10 minute TBS-T washes and incubation with anti-rabbit Alexa 680 (1:50,000, Bio-Red) secondary antibody for 45 minutes at room temperature. Membranes were washed again and were imaged for protein visualization using an Odyssey (LI-COR) imaging system.

2.5. Stereotaxic Surgery

All mice that underwent the stereotaxic injections were weighed and anaesthetised using a mixture of ketamine (130mg/kg; Ketapex; Apex Laboratories, Sydney, Australia) and muscle relaxant xylazine (6mg/kg; Rompun; Bayer, Sydney, Australia). Once anesthetised the mouse was placed on the stereotaxic apparatus (Model 900; Kopf, Tujunga, CA, USA) with the incision bar maintained at -3.3mm below horizontal to allow for flat skull placement. The area where the incision was made was cleaned with an antiseptic betadine.

For *intracerebrovascular (ICV)* injections, the needle was lowered into the lateral ventricles at co-ordinates: A-P 0.0mm; M-L ± 1.0mm; D-V -2.2mm from Bregma. Mice were divided into two groups for each of the two surgery models where they either received a control toxin rabbit-IgG-saporin (0.4µg/ventricle; Advanced Targeting Systems, San Diego, CA) or mu-p75-saporin (0.4µg/ventricle; Advanced Targeting Systems) for the hippocampal degeneration model or a novel neurotoxin, UII-SAP (0.5µg/ventricle; Advanced Targeting Systems) or control toxin, unconjugated SAP (0.5µg/ventricle; Advanced Targeting Systems) diluted in sterile PBS solution for the neurotrophin withdrawal model. The infusions were conducted over 2 mins, with a post injection wait of 5 mins to allow diffusion of the toxin into the ventricles and a slow retraction of the needle over 2 mins. These injections were performed using a 30-gauge needle attached to a 0.5µl Hamilton syringe.

For *medial septum (MS)* injections, a 33-guage needle (C315I/SP; Plastics1) was attached to tubing, which was connected to a 5µl Hamilton syringe on an infusion pump (11plus ADV PUMP; Harvard Apparatus). The needle was lowered into the medial septum at the following co-ordinates; A-P; +1.0, M-L; 0.0mm, D-V; -4.4mm from Bregma. The infusion

was performed over 2 mins, after which the needle was left in place for 8 minutes, retracted 0.5mm and left for additional 2 mins and slowly withdrawn out.

After the surgery, the mice were injected subcutaneously with the analgesic torbogesic (1.3mg/kg) and the antibiotic Baytril (0.43mg/kg). For post surgery care, mice were given another analgesic and antibiotic injection the next day, were weighed daily to record any weight loss and were given mashed food for 3 days post surgery.

2.6. Behavioural Experiments

2.6.1. Passive place avoidance

Mice were subjected to a passive place avoidance behavioural paradigm to test their basal forebrain dependent idiothetic navigation (self-motion kinaesthetic cues). In this navigation task all external cues were eliminated to minimize allothetic navigation (spatial relationships to cues). The apparatus used included a grey opaque arena (80cm diameter, 20cm high) placed on a square grid of parallel metal rods (4mm diameter, 5mm apart) on a stainless steel table 1 meter above the floor. This set up was enclosed in a 2 metre by 2-metre space with grey sound attenuating curtains. The light and sound in the room was maintained and the equipment was cleaned with 70% ethanol before the mice entered the arena.

Mice were placed in the arena directly opposite to the shock zone and were returned to their cage following the trials. On day one, all mice underwent a habituation session where they were allowed to explore the arena freely for 5 minutes without receiving any shocks. After one hour mice went through the training phase of the test where they had to learn to avoid a set 60^{o} shock zone. If the mice entered the shock zone during training, they received a 0.4mV foot-shock for 0.5 second with an interval of 1 second between shocks and an entrance delay of 500ms. To determine their memory of the shock zone, the mice we placed in the arena 24hours later and were allowed to explore without shocks being applied. Mice were tested for 5 minutes for their ability to avoid the shock zone.

In order to analyse the performance, the following parameters were measured: the distance travelled by the mice, the number of entries into the shock zone, the number of shocks received and the homing score (the area the mouse spent the most time in away from the shock zone). The homing score was based on the spread of the area and the fraction of time the mouse spent opposite to the shock zone.

2.6.2. RotaRod

Accelerating RotaRod (UGO Basile Biological Research) was used to the test the motor integrity of mice after surgery for Aim 2b . Mice were positioned on the rotating arm of the RotaRod travelling at 2rpm. The acceleration was set to 0.4rpm/sec up to a maximum of 20rpm. Measurements were made over 180 seconds and the falls prior to 180 seconds were recorded.

2.7. Histological Analysis

2.7.1. Perfusions

Following the delivery of biotin-TAT-c29, mice that were to be used for histological analysis of biotin-TAT-c29 distribution were deeply anaesthetized with a 100mg/kg sodium pentobarbital intraperitoneal injection at each of the time points stated above. The mice were then transcardially perfused with 25mls of Phosphate Buffer Saline (PBS 1X, pH 7.4) followed by 50mls of 4% paraformaldehyde in 0.1M phosphate buffer (PB), pH 7.4. The brain and the spinal cord were dissected out and post fixed in 4% PFA. Brains were post fixed overnight at 4^{o}C while the spinal cord was post fixed for 45 mins at room temperature. Post fixation, the brain and spinal cord were thoroughly washed in PBS before placing them in 20% sucrose solution overnight for cryoprotection. Brains were sectioned using a sliding microtome (SM2000r; Leica, Sydney, Australia) at 40µm coronal thickness in three serially adjacent sets. These sections were stored in 0.1% sodium azide in 0.1M PBS. Spinal cords on the other hand were embedded in OCT (Optimal Cutting Temperature embedding medium) and were frozen using dry ice and cold ethanol. These specimens were stored at -80^{o}C until they were ready to be sectioned coronally on the cryostat at 20µm thickness into five series.

2.6.2. Peroxidase Immunohistochemistry

The peroxidase immunohistochemistry experiments were performed by repeatedly washing the sections in 0.1M PB, followed by one 30 minute 50% ethanol and a 30-minute 50% ethanol and 3% hydrogen peroxide (H_2O_2) wash. The sections were blocked in 5% normal horse serum in 0.1M PB for 30 minutes before they were incubated with the primary antibodies (Refer to Table 2.1) for 48 hours at 4^{o}C diluted in 0.1M PB with 2% horse serum and 0.1% Triton X-100. The sections were then washed 3 times with 0.1M PB and probed with secondary antibody at room temperature overnight (either with the

biotinylated donkey anti-rabbit, biotinylated donkey anti-mouse or biotinylated donkey anti-goat at 1:1000; Jackson Immunoresearch Laboratories, West Grove, PA) diluted in 0.1M PB with 0.1% Triton X-100. After washing excess secondary with 0.1M PB, next day the sections were then incubated for 2 hours at room temperature in ABC reagent (Vector Elite kit: 6 µl/ml avidin and 6 µl/ml biotin; Vector Laboratories, Burlingame, CA). To achieve the dark immunoreactivity, a nickel intensified diaminobenzidine reaction was performed whereby sections were first incubated in 0.1M sodium acetate buffer for 20 minutes followed by a 15 minute incubation in DAB solution (comprising of 0.1M acetate buffer, 2% nickel sulphate, 0.2% D glucose, 0.04% ammonium chloride and 0.025% 3,3-diaminobenzidine). Adding glucose oxidase enzyme (0.2µl/ml) then started the peroxidase reaction, which was stopped with 0.1M acetate buffer solution (pH 6.0). The sections were repeatedly washed in 0.1M PB before mounting they were mounted onto chrome-allum treated slides. Slides were then dehydrated in 100% ethanol twice (3 minutes/ wash), cleared twice in Xylene and coverslipped with DePeX (Distrene-80/plasticizer/xylene; Crown Scientific, Sydney, Australia). The slides were then scanned on the Zeiss Axio Imager Z1 and analysed using the Imaris software (v7.5, Bitplane).

2.7.3. Thioflavin

Thioflavin S stain was used for the detection of amyloid beta plaques for Aim 2c. To perform this staining, 40 um hippocampal slices were first mounted onto slides in order from anterior to posterior. The slides were cleaned twice in dH2O (5mins/wash), then placed in filtered 0.5% Thioflavin S solution made in dH2O for 5 mins and then washed in 70% ethanol for 5 minutes. The slides were then incubated with Dapi nuclear stain (1:5000) made in 0.1%Triton-X for 4hours at room temperature. The slides were washed in PBS 3 times then rinsed twice in dh20 and coverslipped using DAKO (S3023) aqueous mounting medium.

Primary Antibodies	Bright-field IHC	Western Blotting	Company
Goat anti ChAT (Acetylcholine Transferase)	1:1000	-	Jackson Laboratories
Mouse anti Parvalbumin	1:1000	-	Millipore
Rabbit anti 9992 (Intracellular p75NTR)	1:1000	1:1000	Huber & Chao, 1998
Rabbit anti Phospho-p44/42 MAPK (Erk1/2)	1:700	1:1000	Cell Signalling – 9101S
Mouse anti GFAP (Anti-Glial Fibrillary Acidic Protein)	1:50000	-	Dako
Anti-Human p75NTR pAb	-	1:1000	Promega
Anti-p75NTR (Neurotrophin Receptor) Antibody	-	1:2000	Millipore – 07476

Table 2.1 – List of primary antibodies used for immunohistochemistry and western blotting

2.8. Cell Quantification and Imaging

Basal forebrain ChAT cell positive counts were performed for Aims 1a, 1b, 1c and 3 and Mesopontine nuclei ChAT cell counts were performed for Aim 1b. All counts were manually quantified on 20x magnification images whilst being blind to treatment, age or genotype. Bilateral counts of ChAT immunoreactive cells were conducted through the rostro-caudal extent of 120µm apart sections.

For the basal forebrain three different nuclei were identified and counted: medial septum (MS), vertical diagonal band (VDB) and horizontal diagonal band (HDB). In the mesopontine tegmentum two nuclei were quantified: laterodorsal tegmentum (LDT) and pedunculopontine tegmentum (PPT) All nuclei were identified and defined according to the Mouse Brain in Stereotaxic Coordinates Atlas (Franklin and Paxinos, 2007).

Peroxidase stained sections were imaged using a Metasystems bright field slide scanner (Zeiss Azio Imager Z2 microscope). The slides were first prescanned at 5x magnification and the final images were obtained in three Z-stacks using a 20x magnification objective lens. Images were processes and analysed using Imaris 7.5 software (Bitplane Scientific Software). The positively stained cells were counted using the “Spots” application on Imaris.

Counts for the Thioflavin stained hippocampal sections were performed manually using an Upright Zeiss Axio Imager Z1 under a 40x objective lens. Green fluorescence indicating the Aβ plaques were counted along the rostral to caudal axis bilaterally along the hippocampus in 240um apart 40um thick sections.

2.9. Statistical Analysis

Quantitative data was analysed using GraphPad Prism 5 for Mac OS X software (GraphPad Software, Inc). To analyse the effect of surgery/treatments on cell counts and behaviour, a one-way ANOVA was performed for the comparison of the mean cell count (±SEM) between different groups.

Chapter 3 - Models of degeneration to test the efficacy of c29

3.1. Introduction

Based on *in vitro* experiments which demonstrate that c29 can inhibit cell death (Coulson et al., 2000a, Matusica et al., 2013). The Coulson group next wanted to determine whether c29 fragment of the p75NTR receptor could promote neuronal rescue in context of neurotrophin dependent neurodegeneration.

In particular, I was interested in testing the efficacy of biotin-TAT-c29 in an AD model, where as others in the laboratory aimed to test biotin-TAT-c29 in other degenerative models that $p75^{NTR}$-death signalling had been strongly implicated including motor neuron disease. As highlighted in section 1.4, classic AD mouse models do not undergo frank cBF neuron loss. The aim of experiments describe in this Chapter was to investigate other mouse models for their ability to exhibit neurotrophin-mediated degeneration. The three models chosen for investigation were:

(i) the senescence accelerated model of basal forebrain degeneration,
(ii) a neurotrophin withdrawal model of cholinergic basal forebrain degeneration
(iii) Aβ hippocampal degeneration model

3.2. Senescence accelerated model of basal forebrain degeneration

3.2.1. Background

The senescence accelerated mouse (SAM) model is a model of accelerated aging established through phenotypic selection of mice from an inbred genetic pool of the AKR/J strain of mice (Butterfield and Poon, 2005). This resulted in SAM model mice which include nine senescence-accelerated mouse prone (SAMP) sub-strains and three major senescence-accelerated mouse resistant (SAMR) sub-strains, each of which exhibit specific aging related phenotypes (Takeda et al., 1981).

Our interest focussed on the SAMP8 strain which displays a number of features typical of early pathogenesis of AD such as learning and memory impairment, increased oxidative stress, cholinergic deficits, anxiety, age dependent Aβ deposition, and changes in membrane lipids and circadian rhythm disturbances (Flood and Morley, 1993, Butterfield et al., 1997, Miyamoto, 1997). Due to these features, the use of SAMP8 mice in gerontology research, especially dementia, has increased.

The mechanism of age related cognitive decline in these mice is still not entirely clear but studies have attributed it to genetic alterations encoding proteins related to neuroprotection, signal transduction, protein folding, protein degradation, immune response and reactive oxygen species production (Butterfield and Poon, 2005). Evidence suggests oxidative stress and abnormal APP and Aβ metabolism to be the primary cause of learning and memory deficits in SAMP8 mice. It has been reported that increased Aβ accumulation occurs in the hippocampus of these mice and is associated with increasing age (Del Valle et al., 2010, Manich et al., 2011). In addition, administration of antisense oligonucleotides directed against APP to aged SAMP8 mice resulted in an improvement in cognition in association with a reduction in Aβ-induced oxidative stress (Kumar et al., 2000, Poon et al., 2004). The age related abnormalities in this model together with the link between Aβ accumulation and cognitive deficits indicate that the SAMP8 mouse model could be a useful animal model of Alzheimer's disease.

In particular, our interest in the SAMP8 being a model of neurodegeneration to test the efficacy of biotin-TAT-c29 peptide arose from data showing a cholinergic deficit in the basal forebrain region of the SAMP8 mice at 6-8 months of age (Strong et al., 2003, Matsui et al., 2009). This supported the *cholinergic hypothesis* of AD, which proposes that

the cognitive decline noted in aging and AD brains is due to the dysfunction of acetylcholine-containing neurons of the forebrain.

However, although Matsui et al, showed an apparent rescue of the basal forebrain neurons with magnolol and honokiol treatment, the results regarding survival of cBF neurons were difficult to interpret. SAMP8 mice were treated at 2 months of age for 14 days. Mice were analysed at 6 months of age and displayed an increased number of cholinergic neurons at 6 months compared to untreated 2 month old SAMP8 mice (Matsui et al., 2009). The number of ChAT-positive cells in treated SAMP8 mice were also comparable to that of the SAMR1 control strain. However, these results suggest that rather than rescue of cholinergic neuron death, the expression of ChAT per cell was altered, and/or that there was a strain difference in either ChAT expression or absolute cholinergic neuron number between the two strains.

My first aim was therefore to determine if cholinergic neurons degenerated in SAMP8 mice and the period of time during which this occurred. Once defined, animals could be treated over that time period with biotinylated c29 peptide to determine whether the treatment inhibited the degeneration.

3.2.2. Results

Based on the report that that the basal forebrain of SAMP8 mice contain 50% fewer ChAT neurons at 6-8 months of age when compared to the SAMR1 control mice, the strain which is commonly used as controls for SAMP8 mice (Strong et al., 2003), we analysed mice at 3, 4, and 6 months of age. Mice were perfused and processed for histological analysis. Counts of ChAT –positive neurons in the basal forebrain were performed for animals at each time point. As our subsequent treatment design was to compare c29-treated and control-treated SAMP8 mice over a time period, we did not use the SAMR1 for comparison but compared the results longitudinally. Our positive control for the immunostaining was wildtype C57bl6 animals.

The analysis revealed that SAMP8 mice had significantly fewer ChAT-positive basal forebrain neurons compared to C57Bl6 animals but that there was no significant age-related decline in ChAT cell number between 3 and 6 months in the SAMP8 animals (Figure 3.1).

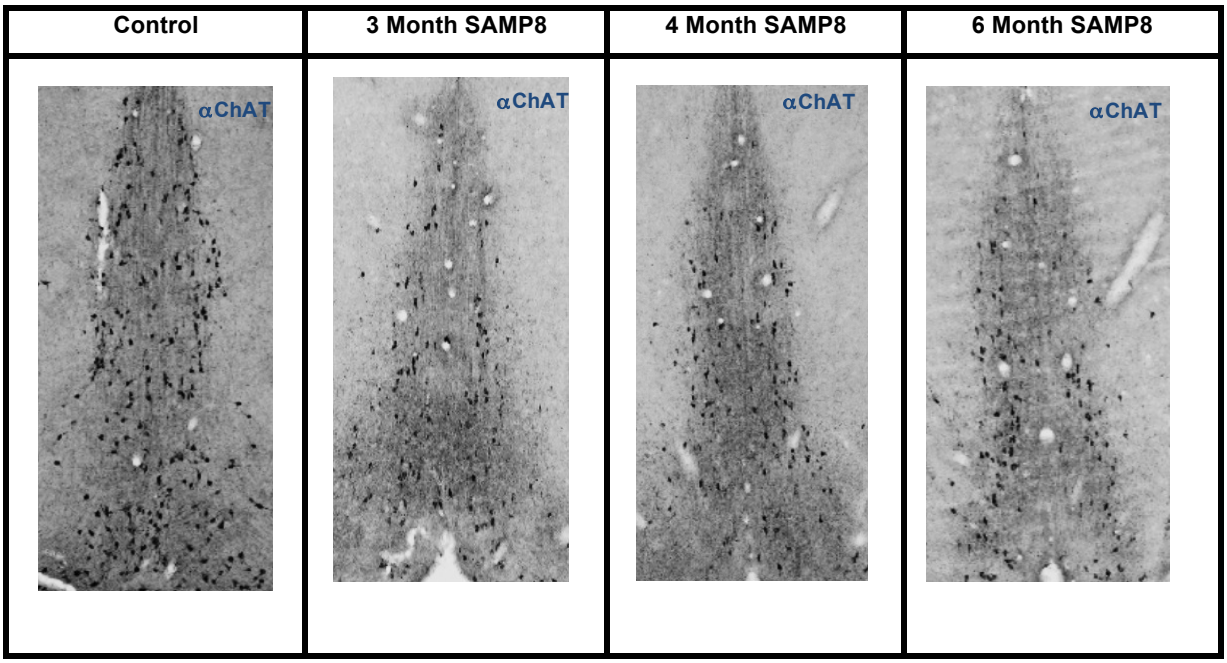

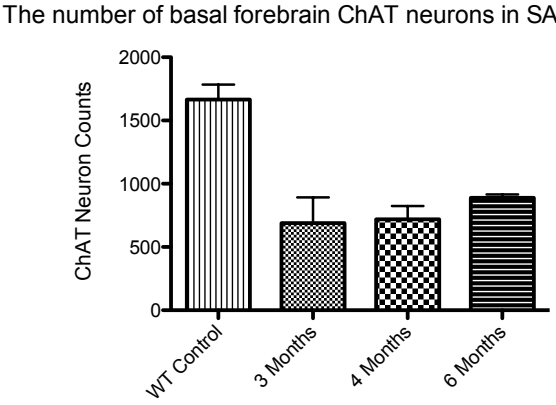

Figure 3.1- Number of ChAT neurons in the basal forebrain region of SAMP8 mice at 3, 4 and 6 months of age

Photomicrographs show ChAT-positive neurons in the basal forebrain of SAMP8 mice of ages 3, 4 and 6 months compared to a c57/Bl6 WT control. The ChAT-positive neurons in the basal forebrain were counted as shown in the graph. The SAMP8 mice had significantly lower ChAT counts than the controls (p=0.01), however there was no significant difference between the ChAT counts of different ages of SAMP8 mice (p=0.58, n=2 per group).

Based on these preliminary investigations, SAMP8 mice did not display an age dependent loss of ChAT-positive neurons in the basal forebrain between 3 and 6 months of age (figure 3.1). While SAMP8 mice have ~50% fewer cholinergic basal forebrain neurons compared to C57Bl6 animals, this deficit did not occur in an age dependent fashion, at least post adulthood (figure 3.1).

In support of this conclusion, immunohistochemistry analysis had also revealed a significant difference in the brain morphology of these mice compared to controls. Firstly, the size of the lateral ventricles were much smaller in the SAMP8 mice. Secondly, despite being stained in the same batches as the C57Bl6 sections, the intensity of the ChAT immunostaining was fainter compared to controls with less positive cells not only in the basal forebrain but also in the striatum (which contains cholinergic interneurons).

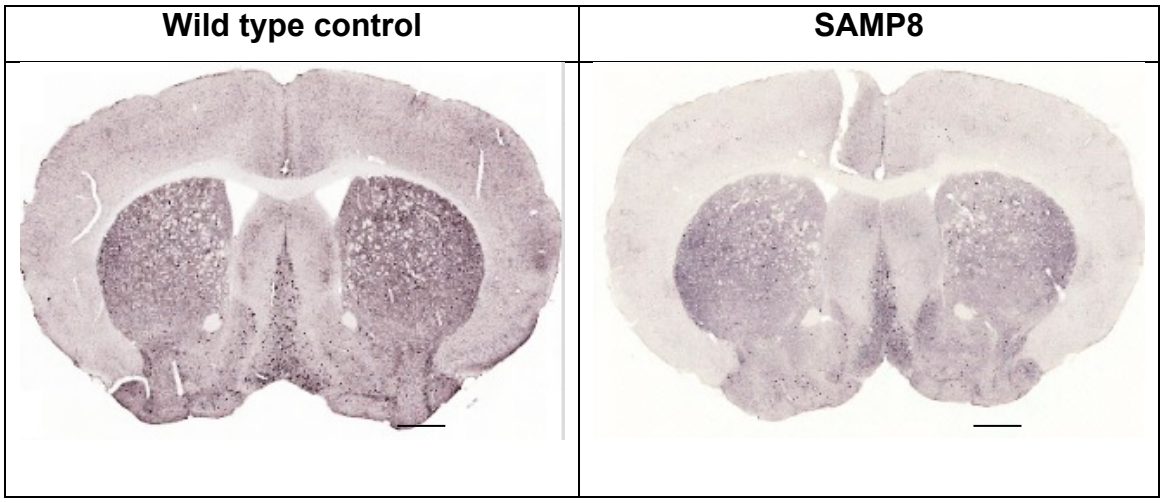

Figure 3.2 - The brain morphology of SAMP8 mice is different when compared to wild type control
2x photomicrographs shows coronal section at the level of the basal forebrain of a 3 month old control and SAMP8 mouse stained with the ChAT antibody (n=2, scale bars 1mm)

3.2.3. Discussion

The primary goal of these experiments was to characterise the time course of cholinergic degeneration in the SAMP8 mouse model to determine its suitability to be used as a model to test the efficacy of the c29 peptide in preventing cholinergic basal forebrain neuronal degeneration.

We did not observe a reduction in the basal forebrain number with age between 3 and 6 months of age of SAMP8 mice. This is in agreement with the Matsui et al study where there was no significant reduction in ChAT-positive neuron number between untreated mice aged 2 months and 6 months of age. (Matsui et al., 2009). However, a previous publication reported an age related change in the ChAT activity between SAMP8 mice age 4 months and 8 months (Strong et al., 2003). This difference could be due to the fact that this paper used ChAT enzymatic activity as a measure of function, as opposed to counting the number of ChAT positive neurons in the basal forebrain. This also suggests the result

of Matsui et al., may be due to a decline in cholinergic function rather than neuron number *per se*.

Thus far, no publication has reported ChAT–positive neuron number levels at 1-2 months of age in these mice. However, we speculate that the reduced cholinergic cell number is due to altered development. It is possible that SAMP8 mice have reduced ChAT expression from birth with a further decrease seen in the level of ChAT activity between 4-8 months.

As our primary outcome measure with c29 treatment was to be neuronal survival, our choice of counting ChAT positive neurons through immunohistochemistry was more relevant to our goal. Similarly, while we could analyse mice younger than 3 months, any change in ChAT neuron number would not be old-age dependent and therefore this would not be the ideal model to test the efficacy of biotinylated c29 peptide. Although this mouse model is not sutiable for the purpose of our study, that the SAMP8 mice apparently have age-related reduction in ChAT activity could make these mice an excellent model for studying cognitive decline and aging.

3.3. Neurotrophin withdrawal model of cholinergic basal forebrain degeneration

3.3.1. Background

The cBF contains the largest population of cholinergic neurons in the brain and is implicated in cortical activation, attention and memory. Degeneration of basal forebrain neurons also occurs in neurological disorders including Alzheimer's disease, Parkinson's disease and schizophrenia (Zabroszky et al, 2012). The cholinergic neurons of the basal forebrain project to various areas of the brain: including the cortex, the hippocampus and the amygdala as illustrated in the schematic below (Figure 3.3).

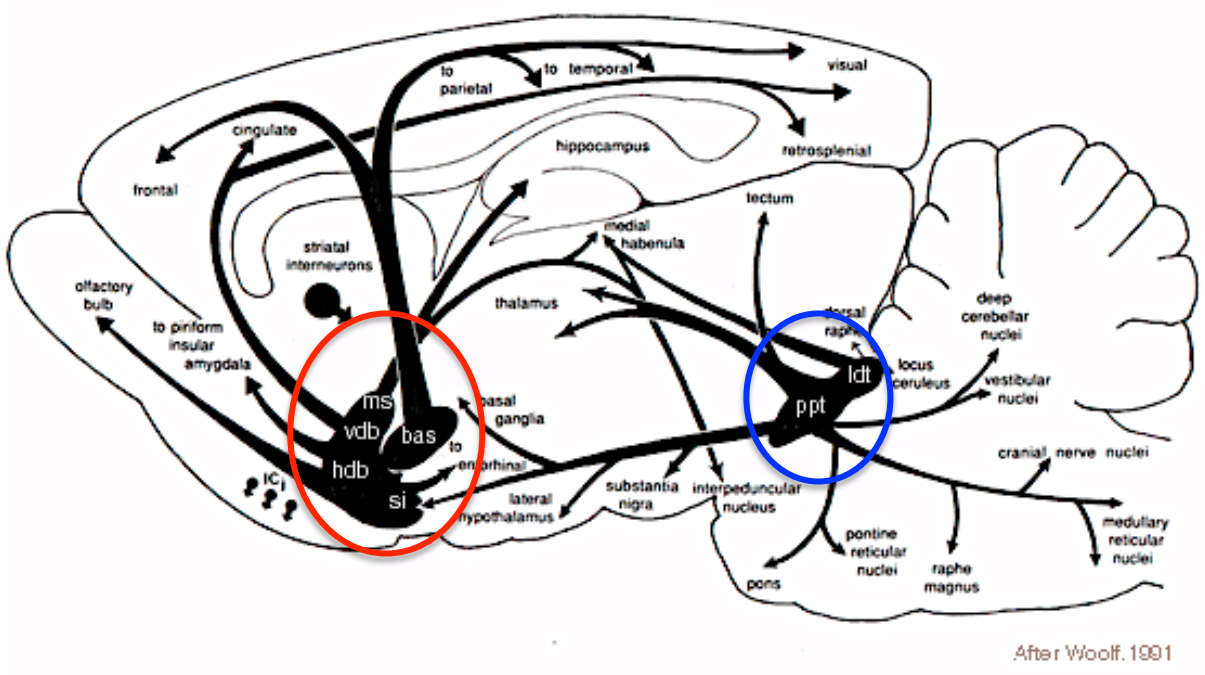

Figure 3.3. - Schematic shows the major cholinergic populations and their projections in the brain (Woolf, 1991)

The largest population of cholinergic neurons in the brain is in the basal forebrain (red) which comprises of the Medial Septum (MS), Vertical Diagonal Band (VDB) and Horizontal Diagonal Band (HDB). The second largest population is in the mesopontine tegmentum (MPT) area located in the peduncular pontine (blue) which comprises of the laterodorsal tegmentum (LDT) and the pedunculopontine tegmentum (PPT). Lastly, the third cholinergic nuclei are the interneurons of the septum.

Our main interest for this aim was to investigate the MPT which comprises of two nuclei: the laterodorsal tegmentum (LDT) and the pedunculopontine tegmentum (PPT). MPT neurons innervate the basal forebrain and other important thalamocortical regions known

to regulate REM sleep (Woolf and Butcher, 1986, Woolf et al., 1990). It has been previously postulated that REM sleep disruptions can exacerbate cognitive decline in AD.

A project was initiated in the Coulson and Bellingham labs to investigate the link between MPT and cBF dysfunction and disrupted sleep in AD. Preliminary data from that study showed a surprising link between ablation of the mesopontine tegmentum (MPT) cholinergic neurons in the midbrain and a loss of the cBF neurons in the medial septum. We hypothesised it was due to a dependence of cBF neuron on supply of NGF from the MPT cholinergic innervation for their survival. It is well established that cBF neuron is dependent upon NGF/TrkA signalling for survival and reduced levels of NGF and or TrkA are associated with AD (Mufson et al., 1997, Capsoni et al., 2000). Furthermore cBFN degenerate when NGF supply is eliminated (Mufson et al., 1997, Capsoni et al., 2000, Fahnestock et al., 2001). Recent evidence suggests that the LDT cholinergic neurons of the MPT produce NGF, raising the possibility of the dependence of medial septum cholinergic population on MPT derived NGF for survival rather than cortical derived NGF (Ramos et al., 2011).

For this aim of my project we wanted to confirm that loss of LDT neurons resulted in degeneration of cBF neurons. To lesion the LDT neurons, we used a toxin in which saporin is conjugated to an Urotensin II receptor peptide. This peptide can be specifically taken up by and kill only neurons expressing Urotensin II receptor-expressing neurons (Huitron-Resendiz et al., 2005, Jegou et al., 2006). The specificity of the Urotensin-II receptor to the MPT cholinergic neurons has previously been demonstrated in rats; using in situ hybridisation, Urotensin-II receptor mRNA was found to be expressed only in MPT region and co-localised with ChAT (Clark et al., 2001). Binding sites for the Urotensin II peptide throughout the brain have also been analysed revealing that the highest level of UII-receptor was the cholinergic mesopontine area (Clark et al., 2001).

The experiments for this aim were designed on the basis of preliminary data obtained from an honours student (Nicola Marks, Honours thesis, 2012) who reported a significant 37% ($n=3$; $p>0.05$) reduction in the number of MS cBF neurons following MPT UII-Saporin injection coincident with a 67% MPT cholinergic neuron lesion ($p>0.001$ $n=3$).

3.3.2. Results

In order to replicate the previous findings and therefore validate the use of this toxin for specifically lesioning MPT cholinergic neurons, the paradigm was repeated using a large cohort of c57/Bl6 wild type mice (12 per group). Mice were injected with either IgG-Saporin control or UII-saporin target toxin. Three weeks after surgery, mice were sacrificed and ChAT counts of the LDT nuclei of MPT and the MS nuclei of the histological sections containing the basal forebrain were preformed. UII-saporin toxin injected animals showed a 44% decrease in the cholinergic neuron number in LDT and a significant 26% decrease in the cholinergic neurons of MS region in the basal forebrain (Figure 3.4.).

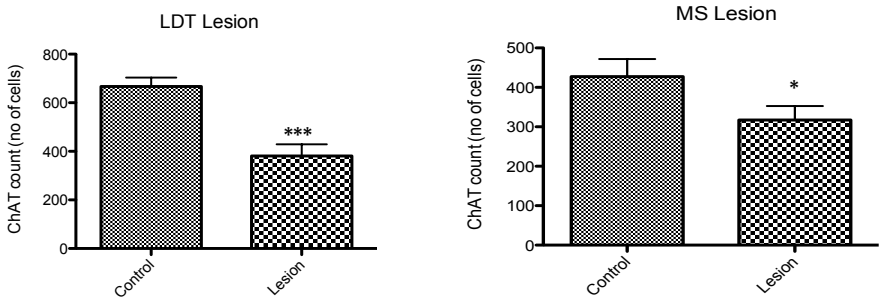

Figure 3.4. - Loss of ChAT neurons with UII-saporin toxin in the LDT and MS

ChAT-positive neurons counts in the laterodorsal tegmentum nuclei of the mesopontine tegmentum shows a significant 44% reduction in ChAT neurons with the UII-saporin toxin (n=12, p<0.0001). ChAT positive neuron count in the medial spetum of the basal forebrain also revealed a significant 26% reduction in the ChAT counts in the UII-sap injected mice (n=12 per group, p<0.0351).

To determine whether the loss of neurons in the basal forebrain was cholinergic specific, the number of parvalbumin positive neurons were assessed in the MS, VDB and HDB nuclei of the basal forebrain. No change in GABAergic neuron population was observed (figure 3.5.) suggesting that the toxin selectively ablated the cholinergic neurons.

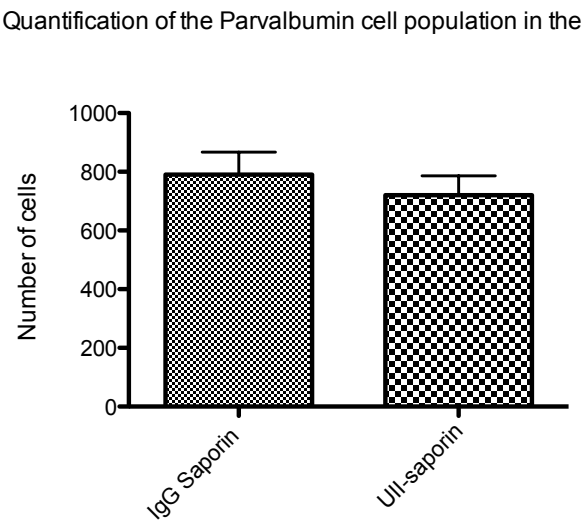

Figure 3.5. - No change of Parvalbumin positive neurons with UII-saporin toxin in the basal forebrain
Quantification of the parvablumin stained GABAergic cells in the basal forebrain of the mice injected with the UII-saporin toxin and the control IgG-saporin toxin did not show a significant difference in the number of cells in each group (n=2 per group).

Prior to sacrifice, these mice also underwent behavioural testing to determine the effect of the lesion on their spatial navigation abilities. Firstly, the mice were tested using the RotaRod, a method of measuring locomotion and coordination, to examine any deficits in motor function as a result of death of cholinergic neurons in the pontine area. No difference between UII-saporin treated and control IgG-saporin treated animals was recorded with all animals remaining on the apparatus for the 3-minute measurement period (Figure 3.6). This result indicated that mice that underwent surgery with the UII-saporin toxin had no substantive motor deficits.

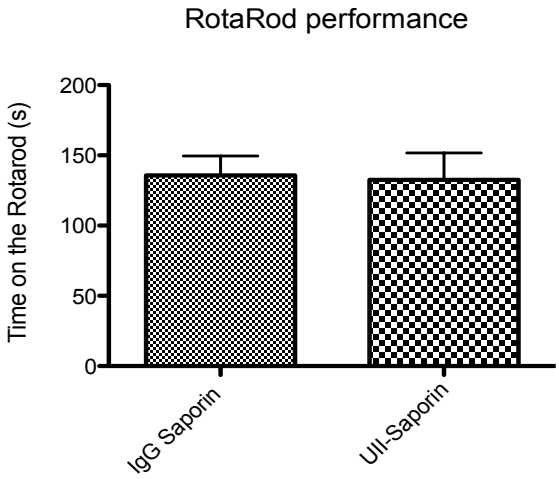

Figure 3.6. - UII-saporin and control injected mice performance on the RotaRod

UII-saporin lesion did not affect the motor performance of mice on the RotaRod task. Both lesioned and control mice performed similarly on the task (n=8 per group, no significant difference in means).

Secondly, mice were subjected to a passive place-avoidance behaviour paradigm which has been validated in the Coulson lab to test for basal forebrain dependent spatial navigation abilities (Hamlin et al, 2013). The performance of the mice in the paradigm was measured in two ways: the number of shocks mice received after training on the paradigm and the homing score for each of the mice groups (Figure 3.7).

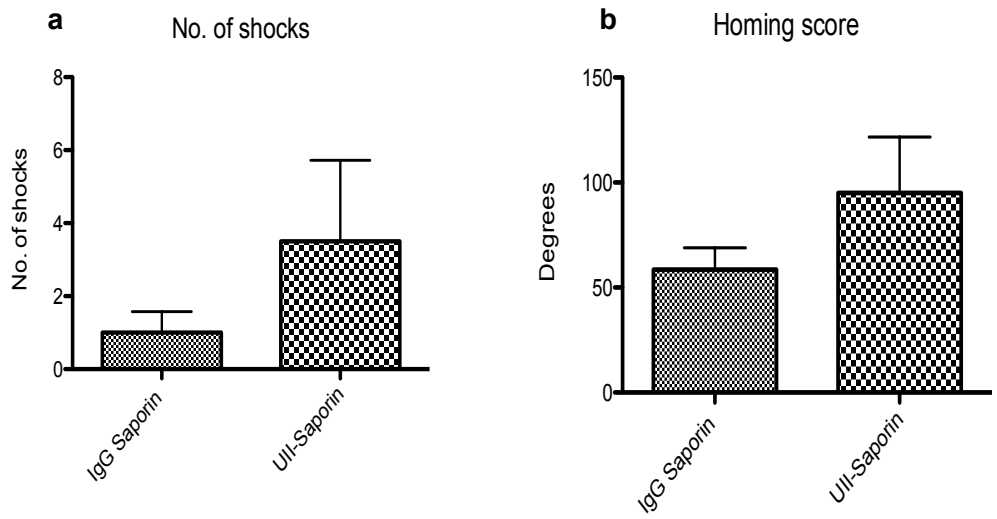

Figure 3.7. - UII-saporin and control injected mice performance on the passive place avoidance paradigm
The data suggested a trend towards impairment in basal forebrain dependent spatial navigation in mice that were lesioned using the UII-saporin toxin (n=8) when compared to the control toxin (n=7) (p=0.1625). Two measures used to analyse the task include: a) No of shocks received and b) the homing angle which is the area measured in degrees that the animal defines as home, away from the shock zone.

Figure 3.7a indicated that there was a trend towards mice lesioned with UII-saporin toxin receiving a greater number of shocks with a significant variability in the number of shocks received by each mouse. This difference in average shock number did not however reach significance. Figure 3.7b indicates the homing angle where a smaller homing score represents the ability of mice to spatially navigate and define a small area as home. Again there was no statistically significant difference, however, the data suggests that the control IgG injected animals defined a smaller area as home compared to UII-sap injected mice which had larger homing scores. These results are consistent with our previous study that loss of cholinergic basal forebrain neurons correlates with impairment in the place avoidance task resulting in greater shock number and larger homing scores (Hamlin et al, 2013).

3.3.3. Discussion

The primary focus of this aim was to validate a model of neurotrophin dependent degeneration which could be rescued using the biotin-TAT-c29 peptide. The approach we took was based on a surprising link found in the lab. In experiments which were aimed at investigating the role of mesopontine tegmentum cholinergic neurons in REM sleep and obstructive sleep apnoea, it was found that ablation of the mesopontine tegmentum cholinergic neurons resulted in the death of medial septum cholinergic neurons of the

basal forebrain. For the purpose of my project, I further examined this association between the two major cholinergic populations of the brain.

The results indicated specific and significant death of medial septum cholinergic neurons in the basal forebrain as a consequence of a lesion in the cholinergic neurons of the laterodorsal tegmentum nuclei of the mesopontine tegmentum area. This loss in the basal forebrain was specific to the cholinergic neurons, as the GABAergic population was not affected. The behavioural data did not reveal any motor deficits in the lesioned mice indicating locomotion controlled by the pontine area was unaffected. By contrast the trend towards spatial navigation impairment suggesting the lesion can result in impairment of a basal forebrain-dependent behaviour task.

This association between LDT and MS has previously been seen by Woolf et al, 1990 where electrical stimulation of MPT resulted in altered density of ChAT staining within the basal forebrain (Woolf et al., 1990). The LDT neuron cholinergic axonal projections comprise of the vast majority of cholinergic innervations from the MPT to the basal forebrain (Woolf and Butcher, 1986, Woolf et al., 1986) and so it is not surprising that loss of cholinergic neurons in MPT region can trigger the loss of neurons in the basal forebrain.

The basal forebrain is dependent on NGF/TrkA survival signalling throughout life and the imbalance in this signalling is associated with Alzheimer's disease (Mufson et al., 1997, Capsoni et al., 2000). Basal forebrain cholinergic neurons have been suggested to derive their survival promoting NGF from targets such as the hippocampus and the cortex to where its projections extend (Gu et al., 1998). Sufficient NGF from these targets is essential for the regulation of basal forebrain plasticity. The loss of cortical NGF reduces the innervation of basal forebrain neurons to the cortex and results in memory impairment. By contrast, enhancing the expression of NGF either exogenously or through repetitive learning tasks increases basal forebrain cholinergic innervation to activated cortical neurons and augments synaptic function and memory (Brooks et al., 2000a, Prakash et al., 2004). Nonetheless, supply of NGF to the basal forebrain cell bodies rather than from the cortex is most potent at keeping basal forebrain neurons alive in the absence of NGF (Hu et al, 1997).

We therefore speculate the reason for the degeneration in the medial septum to be as a result of depletion of NGF produced by the LDT neurons. Since the LDT neurons, which

project to the MS produce NGF (Ramos et al., 2011) its possible that the basal forebrain cholinergic neurons die due sudden loss of NGF positive innervations from the MPT neurons.

Thus far our results indicate that the death of the medial septum neurons is a consequence of the death of LDT neurons. This is supported by literature, as there is no expression of UII-receptor in the basal forebrain (Clark et al., 2001, Jegou et al., 2006). While there is a possibility that the death could be non-specific due to the proximity of basal forebrain to the site of injection (lateral ventricles) we think its unlikely as no change was seen in the parvalbumin GABAergic population, suggesting that the death is ChAT specific. However, in order to completely eliminate the possibility of BFCN death being non-specific, injection of the toxin directly into the MPT region should also be performed. This was attempted as part of this project, however due to the location of the pontine nuclei in the brain, significant optimisation was required to determine the optimal stereotactic injection route.

Future experiments will focus on examining if the death seen in the medial septum is due to loss of trophic support or through another phenomenon occurring as a result of surgery. A possible experiment to examine this would be repeating the surgeries using the UII-saporin toxin in mice overexpressing NGF. Currently, we have a conditional NGF overexpression mouse which uses the cre-lox system. Crossing the NGF mouse to a ChAT-cre mouse will result in overexpression of NGF in all ChAT neurons including the neurons of the basal forebrain and the remaining neurons of the mesopontine tegmentum. If the death seen in the basal forebrain in this model is due a loss of trophic support then in these mice a rescue of basal forebrain cholinergic neurons should be expected.

Another possible way of rescuing the death of basal forebrain neurons is the use of biotin-TAT-c29 peptide. Based on our hypothesis of biotin-TAT-c29 functional mechanism, we believe that in this model, biotin-TAT-c29 will be able to interact with TrkA in the basal forebrain to enhance its activity and compensate for the loss of NGF from the MPT-neurons.

Currently, the behavioural data from this model is non-conclusive despite the presence of a significant basal forebrain lesion. While there was a trend towards basal forebrain impairment using the passive place avoidance task, the data failed to reach significance.

The task should be repeated on a larger cohort of mice. In addition, other navigation tasks such as the Morris water maze could be performed. The medial septum area of the basal forebrain predominantly projects to the hippocampus which is responsible for spatial navigation. Therefore, testing these mice on the morris water maze will examine changes in hippocampal function as a consequence of basal forebrain loss (Catts et al., 2008).

3.4. Aβ hippocampal degeneration model

3.4.1. Background

At a neuropathological level, amyloid plaques, neurofibrillary tangles, progressive synaptic and neuronal loss are the key hallmark features of Alzheimer's disease. Although overexpression and deposition of Aβ appears to be the primary cause of the disease, the basal forebrain cholinergic neuron's vulnerability to the toxicity associated with the disease is not adequately explained. Our lab has recently established a significant correlation between the extent of basal forebrain atrophy and Aβ load in humans as measured by magnetic resonance imaging and a positron emission topography ligand for Aβ known as PiB (Kerbler et al., 2014, submitted). As most APP transgenic animal models fail to show a loss in cholinergic neurons we aimed to establish a 'sporadic' model of AD.

The idea was to establish a causal link between the amyloid accumulation and cholinergic degeneration in AD, specifically to examine if disruptions to normal cholinergic basal forebrain activity would result in the production and deposition of Aβ in the hippocampus. We hypothesised an increase in Aβ plaque production and subsequent hippocampal degeneration would occur following cholinergic basal forebrain neuron lesion. Because mouse Aβ is a different less toxic sequence to that of humans, we used mice susceptible to human Aβ production, the APP/PS1 strain.

This hypothesis was based on a number of previous studies. AD11 mice have reduced endogenous NGF levels due to transgenic expression of an NGF antibody. These animals not only show cholinergic basal forebrain neuron, but also an accumulation of Aβ granules derived from mouse APP (Capsoni et al., 2000, Capsoni et al., 2002). SAMP8 mice also display Aβ accumulation and reduced basal forebrain function which appeared to be linked (Del Valle et al., 2010, Manich et al., 2011). Other evidence from transgenic mice models that supports our hypothesis comes from a paper which looked at Aβ plaque accumulation in p75NTR-knock out mice. This paper found there to be a 20% increase in Aβ plaques deposition by 6 months of age following loss of basal forebrain expression of p75 which binds and can help clear Aβ (Wang et al., 2011). Increased Aβ42 in the brain also occurs when TrkA levels in the cholinergic basal forebrain are low (Hernandez et al., 2010). Together these findings argue that the disruption of cBFN activity and thereby neurotrophin signalling could potentially result in Aβ aggregation and deposition.

In order to investigate this link at a molecular level, we made use of the p75-saporin model of cBF death in APP/PS1 mice. The p75-saporin toxin has been previously characterised in wild type mice whereby intracerebroventricular (ICV) injection of p75-saporin resulted in a specific loss of ChAT positive neurons while preserving other cell population in the cBF (Moreau et al., 2008). As the basal forebrain is one of the only few areas that continues expressing p75NTR in the adult brain post development, we would be specifically targeting the cBFN neurons with this toxin.

3.4.2. Results

Initially, the p75NTR-saporin toxin was tested for its ability to induce a lesion in the cholinergic basal forebrain of 8-week-old APP/PS1 mice. Two weeks post ICV injection of p75NTR-saporin toxin into the lateral ventricles, a significant 34% reduction in the p75NTR positive cholinergic neurons of the basal forebrain was noted (Figure 3.8). These mice were also examined for the number of Aβ plaques in the hippocampus, however in this age group no plaques were seen.

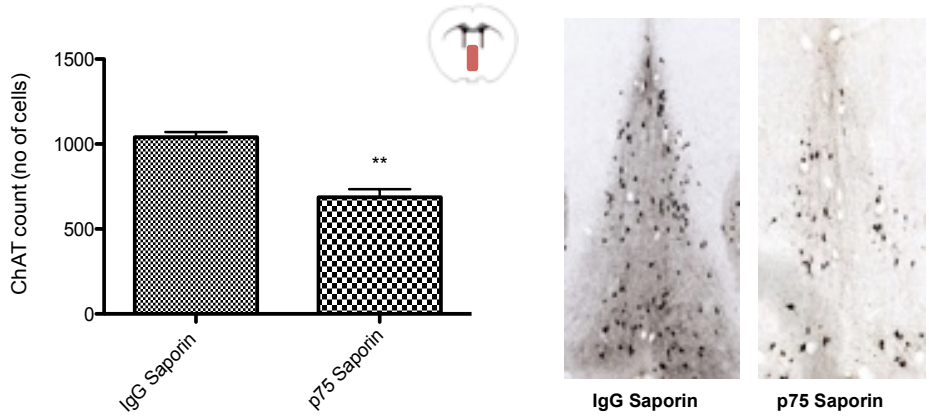

Figure 3.8. - Ablation of p75 expressing ChAT neurons with p75-saporin toxin in APP/PS1 8 week old mice after 2 weeks

Number of ChAT-positive neurons in the basal forebrain of mice 2 weeks after bilateral injection of p75-saporin (n=4) or control IgG-saporin (n=3) were counted. p75-saporin resulted in a 34% loss of cholinergic neurons in the basal forebrain compared to the control condition (p=0.0011).

To test our hypothesis of increased plaque production in the hippocampus as a result of basal forebrain death, further surgeries were performed on mice of different age groups – 8 weeks, 12 weeks and 17 weeks. The 8 week old mice were housed for 2 months after the surgery while the 12 weeks and 17 week mice were housed for 1 month post surgery. At all ages there was a significant reduction in the number of p75NTR-positive cholinergic

neurons of the basal forebrain region. The 17-week-old mice display the biggest reduction of 53.5% in ChAT counts (figure 3.9).

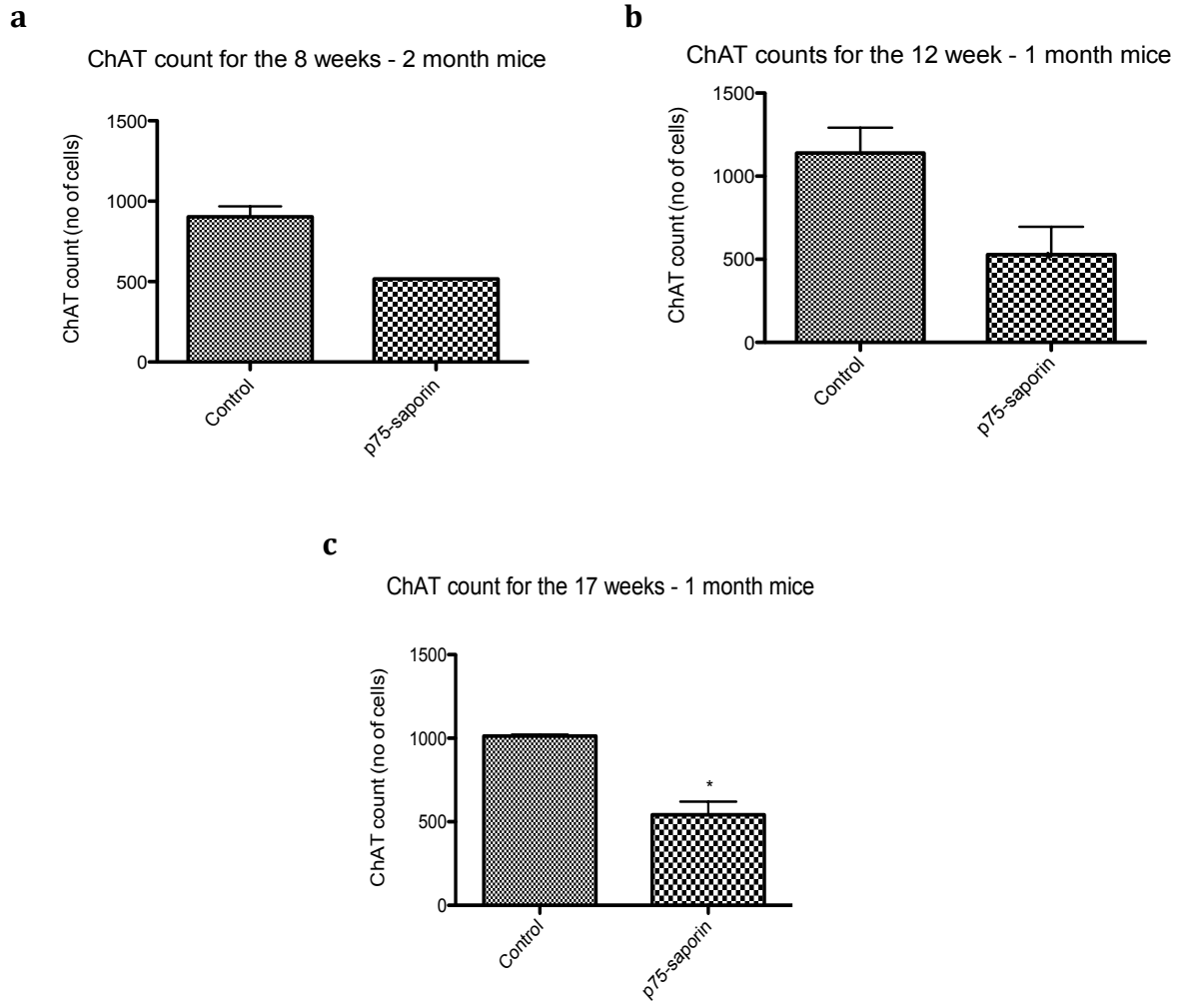

Figure 3.9. - Loss of basal forebrain ChAT positive neurons with p75-saporin toxin at different ages

a) shows a 42.7% loss of cholinergic neurons in the basal forebrain of 8 week old APP/PS1 mice 2 months after bilateral injection of p75-saporin (Statistical analysis could not be performed on this as there is only n=1 in the p75-saporin group). Graph ***b)*** *shows a 46.5% loss of cholinergic neurons in the basal forebrain of 12 week old APP/PS1 mice 1 month after bilateral injection of p75-saporin (n=2) (p=0.0138). Graph* ***c)*** *shows a 53.5% loss of cholinergic neurons in the basal forebrain of 12 week old APP/PS1 mice 1 month after bilateral injection of p75-saporin (n=2) (p=0.03).*

Mice were next examined for the number of hippocampal plaques (figure 3.10.). An increase in the plaque number per hippocampus section was noted for all three age groups. In the 17-week old mice; controls had 6±0.4 plaques/hippocampal section where as the p75-saporin injected animal had 10.4±0.4 plaques/hippocampal section. For the 12-week old mice; the controls had 0.21±0.1 plaques/hippocampal section whereas the p75-saporin injected mouse had 0.77 plaques/hippocampal section. Finally, the 8-week old controls had 0.28±0.1 plaques/hippocampal section compared to the p75-saporin injected mouse which had 2.19 plaques/hippocampal section. At all the ages, basal forebrain ablation using the p75NTR toxin resulted in more Aβ plaques in the hippocampus of APP/PS1 mice than controls (figure 3.10). Statistical analysis was not be performed due to low subject numbers (n=1-2/group

a

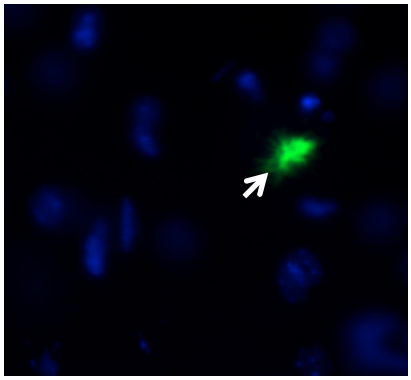

b

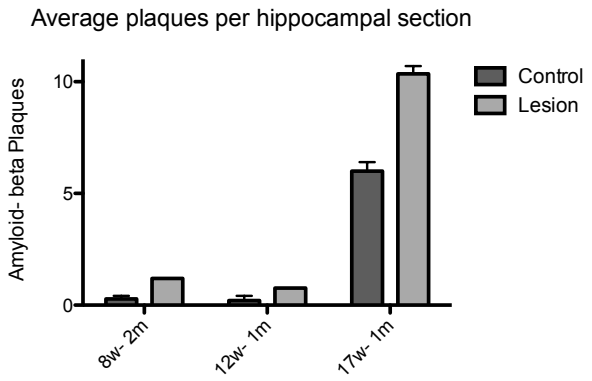

	Control	Lesion
12 weeks	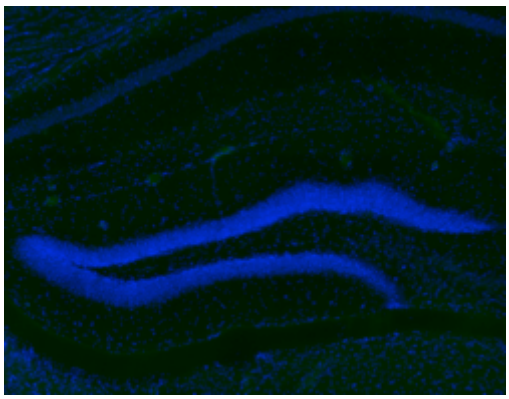	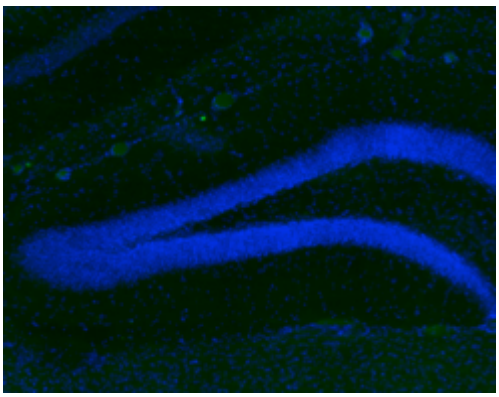
17 weeks	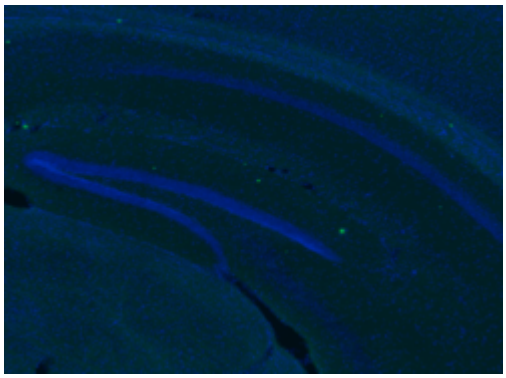	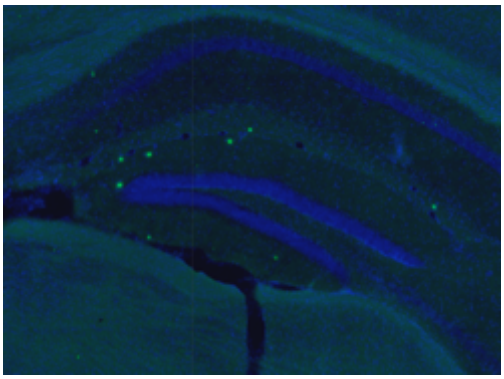

Figure 3.10. - Amyloid beta plaques in the hippocampus of mice post cBF loss

a) shows a 40x magnification of Aβ plaque stained with Thioflavin S. These plaques were counted in every third section through the mouse hippocampus. b) shows the quantification of the increase in Aβ plaque production in the hippocampus of 8, 12 and 17 weeks mice. c) shows the thioflavin S stained photomicrographs displaying the increase in the number of plaque production at 12 weeks and 17 weeks of age (20x magnification, n=2 per group, scale bars 50um).

3.4.3. Discussion

There is strong evidence in support of amyloid beta being the proximal cause of Alzheimer's disease. However, mutations in the amyloid beta protein precursor (APP) gene or the enzymes that cleave the gene to produce a longer form of Aβ only account for less than 10% of cases of AD (Hardy et al., 1998). The overproduction of Aβ and the inability of the brain to degrade it is what leads to the aggregation and accumulation of toxic oligomeric Aβ. The reason for all other sporadic cases of AD is yet to be elucidated. As well as Aβ mediated toxicity, extensive loss of acetylcholine levels and death of the cholinergic neurons of the basal forebrain has been noted in AD (Auld et al., 2002). The cholinergic neurons are responsible for cognitive abilities such as attention, learning and memory processes and its not surprising that their loss results in the main clinical hallmarks of AD.

Early in the disease, degeneration takes place in two main areas: the hippocampus and the basal forebrain. This study was based on a link found in our lab between the load of Aβ in the brain as measure by PiB (Aβ binding tracer used in PET scans) and its correlation with the level of basal forebrain atrophy in humans. We wanted to examine if there was a causal link between the basal forebrain degeneration and Aβ plaque accumulation at a molecular level. We hypothesised that the loss of the cholinergic neurons in the basal forebrain precedes and results in amyloid beta plaque production in the hippocampus and its degeneration.

Currently, there are no models of AD that rapidly develop cholinergic basal forebrain death. In order to test our hypothesis we developed a sporadic model of Alzheimer's disease using the p75NTR toxin in order to examine the effects of basal forebrain death on subsequent degeneration. We were aiming to induce a threshold lesion which would have no or little impact on the normal cognitive functioning of these mice and therefore would allow us to examine the combined effect of basal forebrain loss with the APP/PS1 genotype at a biochemical and behavioural level.

Using the p75NTR- saporin toxin, approximately 50% of all basal forebrain cholinergic neurons and therefore the cholinergic projections to the hippocampus and the cortex were successfully ablated, as reported previously (Hamlin et al, 2013). According to the literature, APP/PS1 mice show Aβ deposition from 4 months of age (Perez et al., 2007). We aimed to exacerbate plaque production with the lesion in susceptible APP/PS1 mice

which according to the literature show Aβ deposition from 4 months of age (Perez et al., 2007). For the mice lesioned at 8 weeks and which had 34% neuron loss at 10 weeks, no Aβ plaques were observed. This could be due to the 34% lesion being too minor to result in significant Aβ production/deposition or the two week timeline being too short to allow for plaque production.

In our next experiment we demonstrated that a robust lesion and prolonged post surgery time was sufficient to aggravate Aβ plaque production in APP/PS1 mice. It was found that lesioning at 17 weeks, resulting in a 50% cholinergic lesion, resulted in a doubling of plaque number in the hippocampus. A similar trend, albeit lower total plaque number was also noted in mice lesioned at 12-weeks of age and lesioned at 8-week but which were housed for 2 months after surgery prior to analysis.

While the aforementioned three studies published recently are in agreement of our model, their experimental design had a few discrepancies compared to ours. Laursen et al and Ramos-Rodriguez et al both used APP/PS1 mice at the ages of 6 and 7 months respectively while Härtig et al used the triple transgenic AD mice at 12 months of age. Laursen et al analysed the mice two months after surgeries and found there to be increase in Aβ plaque, decrease in ChAT activity in the hippocampus and the cortex and significant behavioural impairment (Laursen et al., 2013). Ramos-Rodriguez et al assessed their mice after one week of p75NTR-saporin surgeries and found there to be an increase in Aβ plaques and impairment in episodic memory (Ramos-Rodriguez et al., 2013). Finally, Härtig et al analysed their mice 4 months after lesion and found an increase in Aβ , tau and gliosis (Härtig et al., 2013).

All these studies used mice of an older age group than ours. We wanted to establish the earliest time point before the onset of plaque accumulation where the process could be accelerated by the exacerbation of the cholinergic basal forebrain. We found that at ages as early as 12-weeks we could see a difference in plaque number. Nonetheless, the three studies supported our overall hypothesis and enabled us to conclude that a combination of partial cholinergic lesion and Aβ phenotype represents a novel model which closely resembles the pathophysiology seen early in AD.

One main drawback of our study was the smaller subject groups. Due to the unavailability of APP/PS1 mice at the time of these experiments, the study lacks larger cohorts of mice

and therefore the appropriate behavioural data. Therefore, for the future experiments, a larger cohort of mice is essential to confirm the model at an early age of 12 weeks. However, this model provides us with an excellent degeneration model to test the efficacy of the c29 peptide. Future behavioural analysis should also be performed to comment on the memory and attention impairment in these mice and to examine if c29 treatment is able to prevent plaque accumulation and the subsequent behavioural degeneration.

Chapter 4 - Optimizing delivery of c29 peptide *in vivo*

4.1. Introduction

To test whether biotin-TAT-c29 is efficacious in treating neurodegeneration in one or more of the animal models explored above, it was necessary to optimize a protocol for delivery and detection of c29 *in vivo.* The cellular target of c29 is neurons within the central nervous system (CNS) moreover, in the cytoplasm of those neurons; the hypothesised mechanism of action of c29 is its ability to bind to the intracellular cytoplasmic tail of Trk receptors causing an allosteric change in the receptor structure such that it binds neurotrophins with greater affinity and thereby initiating neurotrophic signalling cascades in concentrations of growth factor lower than would normally elicit such a response (Matusica et al., 2013).

In order to aid intracellular delivery, c29 was coupled to a trans-activating transcriptional activator (TAT) protein transduction domain (PTD) which is a modified version of the PTD4 sequence that has 3-4 times efficiency compared to the wild-type TAT protein sequence (Ho et al., 2004). Firstly this domain delivers peptides and proteins into cells (Schwarze et al., 1999, Coulson et al., 2000a). However and more importantly, PTDs have also been shown to deliver proteins and peptides to a variety of tissues including across the blood brain barrier (BBB), which is well known to be a major hindrance for the delivery of macromolecules into the brain (Schwarze et al., 1999, Gupta et al., 2005). We therefore tested whether c29 can be delivered into the brain following systemic application.

4.2. Results

4.2.1. Intraperitoneal injection of biotin-TAT-c29

To establish delivery of c29 into the CNS, a biotinylated version of TAT-c29 was intraperitoneally injected into mice. Since TAT–coupled peptides could be immunogenic and excessive c29 can potentially enhance signalling resulting in adverse effects, we administered 2mg/kg at different time points to check if any toxicity was caused at this concentration. This dose is the lowest dose of a TAT-coupled peptide previously been reported to elicit biological outcomes in the brain following intraperitoneal delivery of various other TAT peptides (Schwarze et al., 1999, Asoh et al., 2002, Cao et al., 2002, Tao and Johns, 2008, Tao et al., 2008).

Mice injected with biotin-TAT-c29 were sacrificed at 1 hour, 6 hours, 24 hours and 72 hours later following injections. Brain tissue was sectioned at 40μm slices for histological analysis of biotin-TAT-c29 distribution in the brain. We were particularly interested in examining whether biotin-TAT-c29 would be delivered to basal forebrain neurons, which are known to degenerate in AD and the focus of my animal models.

Mice injected with 2mg/kg peptide displayed no noticeable adverse effects within the 72-hour time frame, suggesting that the peptide is not overtly toxic at that dose. Immunohistochemical analysis for biotin-TAT-c29 peptide in brain sections of injected mice compared to naïve mice indicated the presence of biotin within basal forebrain tissue at 1 hour, 6 hours, 24 hours and 72 hours post injection (Fig 4.1). This suggests that the peptide can cross the blood brain barrier within an hour of intraperitoneal injection. Furthermore, immunoreactivity for biotin was still above that of naïve mice at 72 hours, suggesting that the peptide (or its derivatives) are stable for up to 72 hours post injection. This was perhaps surprising given the assumption that peptides have a short biological half-life.

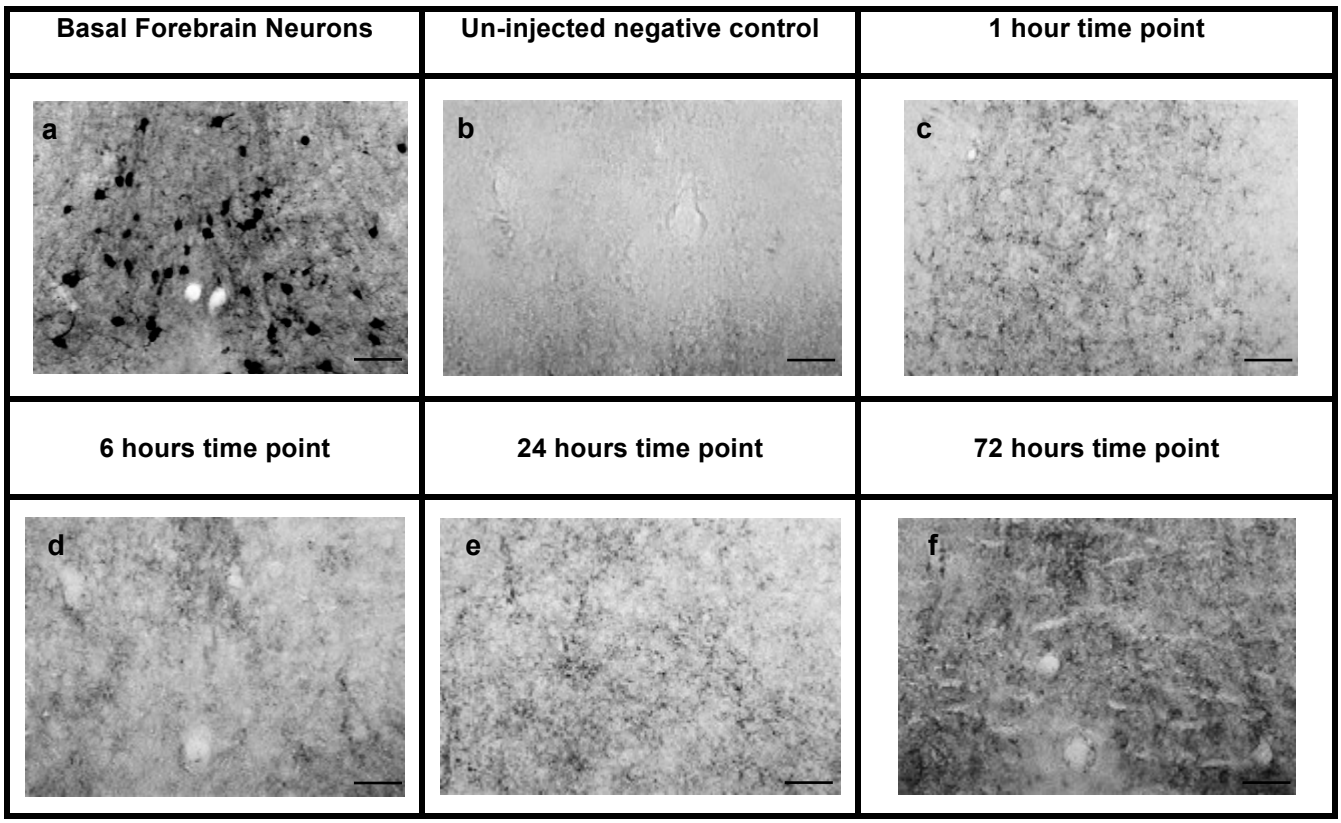

Figure 4.1: Detection of biotin-TAT-c29 in the brain at different time points

Photomicrographs of mouse brain sections at the level of the basal forebrain immunostained with DAB for ChAT (a) or biotin (b-f). Mice injected with the biotin-TAT-c29 peptide (c-f) display positive immunostaining for biotin compared to immunostaining of uninjected mouse tissue (b). All sections were staining and developed in parallel. Immunostanining is evident in sections from all mice injected with biotin-TAT-c29 regardless of analysis time post injection (n=2 animals per time point, scale bars – 50μm, 40X images).

We next tested the amount of biotin-TAT-c29 in the brain following chronic systemic treatment and over an increased range of concentrations; mice were injected with one of three different concentrations of biotin-TAT-c29: 2mg/kg, 5mg/kg or 8mg/kg and injections were given every 72 hours for 6 weeks. Weight of the mice was monitored daily and mice were also observed for any other adverse behavioural responses. At the end of the injection regime, mice were sacrificed and brain tissue processed for histological assessment (figure 4.2.).

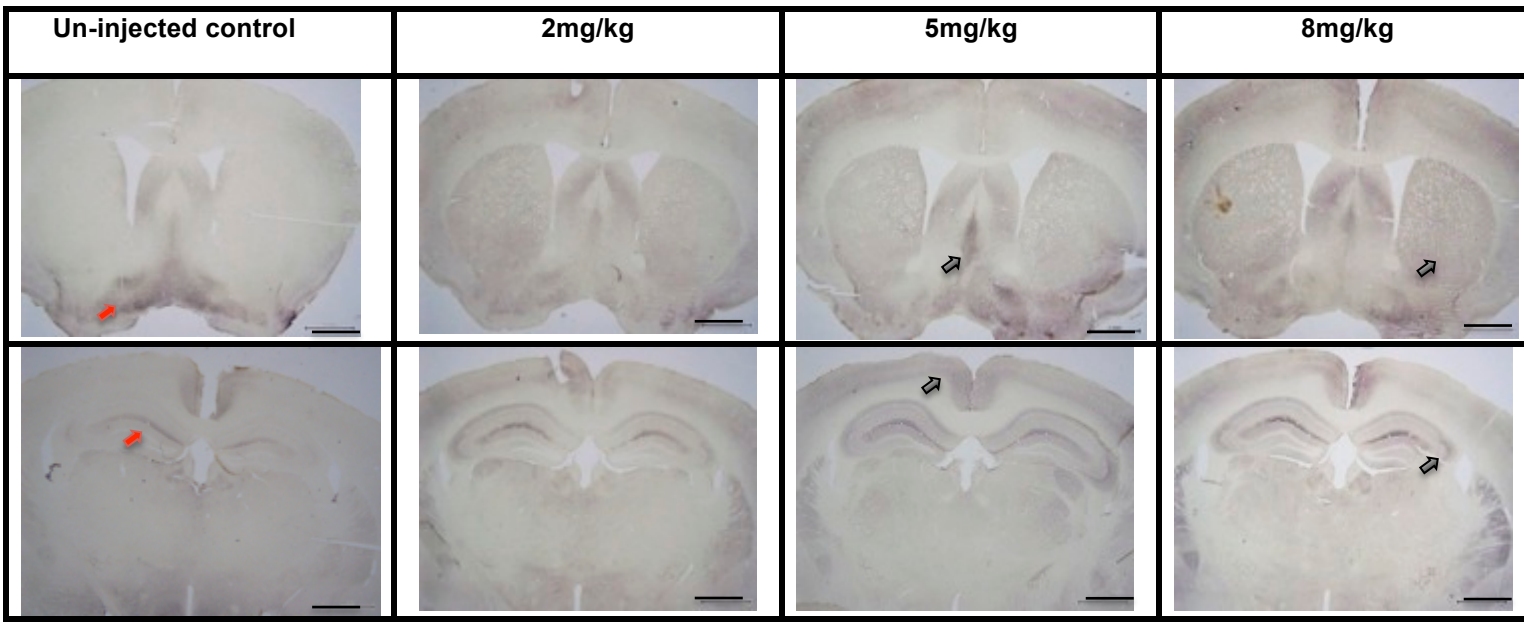

Figure 4.2: detection of biotin-TAT-c29 in the brain at different concentrations using DAB immunohistochemistry

*Panel **a** and **b** show 2x bright field photomicrographs of the basal forebrain and the hippocampal area respectively. The images show the difference in staining for the biotin-TAT-c29 peptide between a non-injected control and mice injected with 2mg/kg, 5mg/kg and 8mg/kg c29 peptide. The black arrows indicate staining above background and higher than negative control (no peptide injected) suggesting the presence of peptide. Red arrows indicate background staining. (n=3, scale bars – 1mm).*

No weight loss was observed and only 1 animal (given the 8mg/kg) appeared to react to the injection (hunched appearance in the corner of the cage immediately post injection) on one occasion during the treatment course. Given the route of administration was intraperitoneal and no other mice were observed to have a similar response, this reaction was assumed to be due to the injection related rather than peptide. We concluded that mice could tolerate up to 8 mg/kg for at least 6 weeks administration of biotin-TAT-c29 peptide with no obvious side effects.

Histological analyses of the brain sections again revealed positive immunostaining for biotin compared with controls (Figure 4.2). Although there was staining observed in the brains of un-injected control mice (indicated by red arrows), immunoreactivity in other brain areas of biotin-TAT-c29-injected mice was not present in the un-injected mouse brains, specifically in the cortex, striatum, basal forebrain and the CA regions of the hippocampus. Interestingly, the immunopositive staining was predominantly associated with grey matter/cell bodies rather than axonal tracks.

The most likely explanation for the staining in the brains of un-injected mouse tissue is the presence of endogenous biotin (McKay et al., 2008). Biotin is a vitamin essential for metabolism and is widely distributed throughout the body, especially in the kidney, liver and brain (McKay et al., 2004). This presence of endogenous biotin can make avidin-biotin and streptavidin-biotin based immunohistochemical detection difficult to interpret. Here the distribution of biotin immunostaining was different in biotin-TAT-c29 treated compared to untreated mice, suggesting the peptide or derivative were transported to the brain. However, although using the avidin-biotin kit confirms presence of the biotin in the tissue, it does not detect the peptide itself, and it was possible that, due to degradation of the peptide, the detected biotin was no longer coupled to the TAT-c29 peptide. Therefore, we next tested whether intact peptide could be detected in cell and tissue lysates.

The first method tested was to immunoprecipiate the biotinylated peptide from lysates using streptavidin-coated beads, followed by Western blotting of elutes with an anti-streptavidin antibody. Lysates from PC12 cells treated with biotin-TAT-c29 and mouse brain lysates spiked with peptide (or naïve) were examined. Eluates were compared by western blot to pure peptide (Figure 4.3). No immunopositive band of ~5kD band, corresponding to biotin-TAT-c29 was detected in any of the lanes including those loaded with different amounts of pure peptide. There were a number of higher molecular weight non-specific bands in pull-downs from both spiked and un-spiked lysates, but again no band that corresponded to the peptide was observed in these samples. It was unlikely that the amount of peptide was below detection limits as 1µg of Aβ peptide – also a 40 amino acid peptide is detectable by western blot (Sotthibundhu, 2009). This suggested that the peptide was not being recognised by the anti-streptavidin antibody following western blotting.

The results taken together indicated that the use of streptavidin-biotin detection was not optimal for detecting biotin-TAT-c29 by immunohistochemistry of tissue sections and was not possible western blotting of tissue lysates.

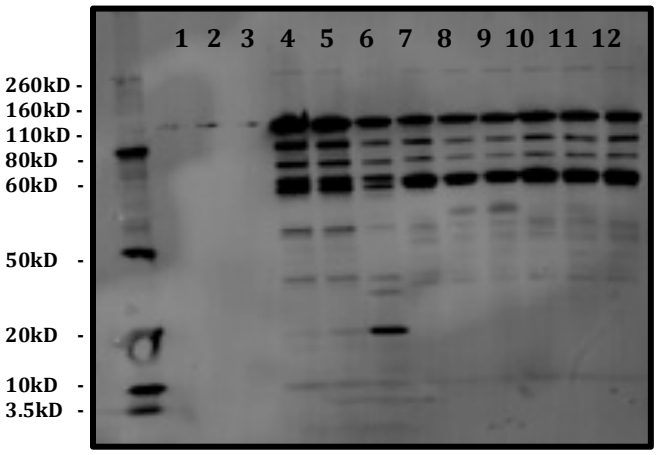

Figure 4.3: Detection of biotin-TAT-c29 peptide by western blot using a streptavidin antibody

*Western blot probed with an anti-streptavidin 680 Alexa-conjugated antibody. Lane **1-3** were loaded with 100, 250 and 500ng of pure biotin-TAT-c29 peptide. Samples in lanes **4-12** are eluates of pull-downs using magnetic streptavidin beads. Lanes **4-6** pull-down from PC12 lysates treated with 10μM, 1μM or control scrambled c29 respectively. Lane **7** and **10:** pull-down of un-injected brain lysate. Lanes **8, 9, 11 and 12** pull-down of brain lysate 'spiked' with 0, 100 and 500ng concentrations of biotin-TAT-c29 peptide, respectively. The expected biotin-TAT-c29 band is ~5kD.*

We next tested whether an antibody to the $p75^{NTR}$ intracellular domain could be used to detect the $p75^{NTR}$-derived c29 portion of the peptide. A number of polyclonal antibodies have been raised to the entire intracellular domain of $p75^{NTR}$, and the c29 sequence is 100% homologous across all mammalian species. These antibodies are routinely used to detect $p75^{NTR}$ and its intracellular domain fragments by western blot and immunocytochemistry. Three different $p75^{NTR}$ antibodies were evaluated for their ability to detect the Biotin-TAT-c29 peptide by western blot: The anti-human $p75^{NTR}$ antibody (Promega, G323A), the anti-NGF Receptor $p75^{NTR}$ antibody (07476, Millipore), both of which are commercial antibodies, and the anti-p75NTR 9992 antibody, generated by Moses Chao (Huber and Chao, 1995) and used routinely for immunoprecipitations and was a generous gift. Western blots of pure biotin-TAT-c29 peptide indicated that only 9992 recognised the peptide (Figure 4.4).

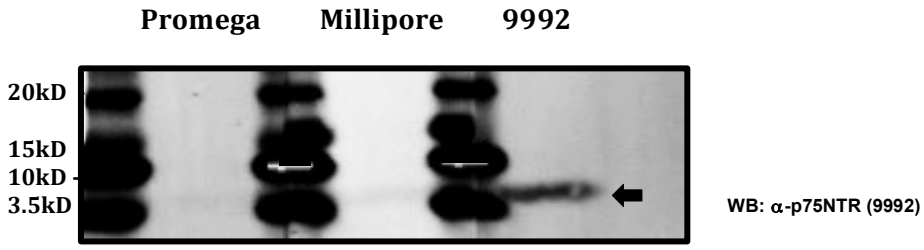

Figure 4.4. - Detection of biotin-TAT-c29 peptide by western blot using the p75NTR intracellular (9992) antibody

Western blots of pure 500ng peptide probed with one of three different antibodies Only 9992 detected a band at the expected 5kD size of the peptide.

The ability of only the 9992 intracellular p75NTR antibody to detect the biotin-TAT-c29 peptide on a western blot could be due to the ability of antibodies to bind only specific conformation of p75NTR/c29 peptide and/or due to the fact that each of the polyclonal populations of antibodies contain antibodies to different epitopes and only 9992 contains an antibody to the c29 region of the p75NTR intracellular domain.

Next, we spiked various amounts of biotin-TAT-c29 peptide to brain lysate from naive animals ('spiked' lysate) and the lysate was then incubated with streptavidin magnetic beads. In this method, biotin-TAT-c29 but not endogenous full-length p75NTR should be retained. The pulldown eluate was then probed using the 9992 antibody following western blotting which revealed biotin-TAT-c29 peptide can be purified from brain lysates and detected by western blot (Figure 4.5).

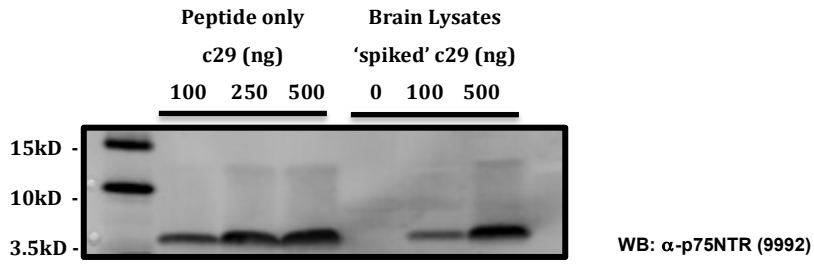

Figure 4.5. - varying concentrations and immunoprecipitation of c29 peptide could be detected on a western blot with the p75NTR intracellular (9992) antibody

Lane 1 shows the ladder. Lane 2-4 show biotin-TAT-c29 peptide loaded at different concentrations of 100ng, 250ng and 500ng. Lane 5-7 show brain lysates spiked with the c29 peptide at 0ng (control), 100ng and 500ng and then immunoprecipitated with streptavidin magnetic beads for biotin-TAT-c29.

No bands were seen in the control un-spiked brain lysate lane indicating that the pull-down was specific for the peptide. The results from this experiment also indicate that the density of biotin-TAT-c29 peptide detected on western blots following pull-down using streptavidin is reflective of the amount of peptide within the lysate. The band intensity correlates with the amount of peptide spiked into the lysate.

Having established a method to detect the c29 portion of the peptide, we tested whether peptide in brain lysates from mice injected with the biotin-TAT-c29 peptide could be observed using this method. Whole brain lysates from mice treated for 1 hour previously with 2, 5 or 8mg/kg biotin-TAT-c29, or for 1, 6, 24 or 72 hours with 2mg/kg were mixed with magnetic streptavidin beads to bind the biotinylated c29 peptide. The eluate from the beads was electrophoresed, western blotted and probed with the 9992 antibody (Figure 4.6.).

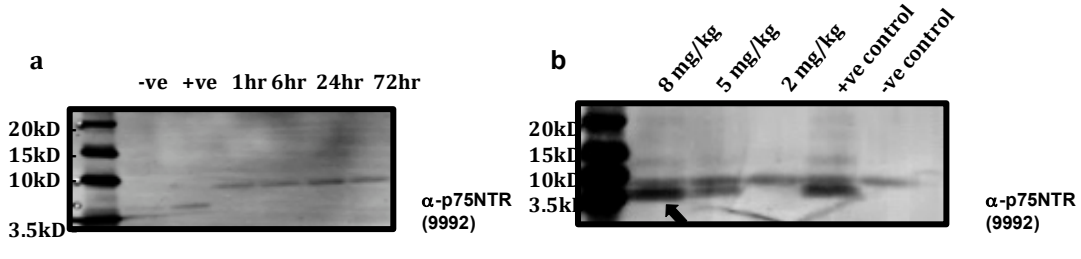

Figure 4.6. - Detection of c29 peptide in brain lysates by western blotting with the p75NTR intracellular (9992) antibody following streptavidin pulldown

(a) Western blot of pull-down eluates from brain lysates of mice were sacrificed at the indicated time point after a single i.p injection of 2mg/kg biotin-TAT-c29 peptide probed with 9992. (b) Western blot of pull-down eluates from brain lysates of mice treated for 6 weeks with 2, 5 or 8 mg/kg biotin-TAT-c29 and sacrificed 1 hour after the last i.p injection, and probed with 9992. A non-specific band larger than that of the positive-control peptide can be seen at ~7Kda. In animals treated chronically with 5 or 8mg/kg a 4Kda band equivalent to the positive control is observed. No band is observed in samples from mice treated with 2mg/kg either acutely or chronically.

This experiment indicates that intraperitoneal injection of 2mg/kg biotin-TAT-c29 did not deliver sufficient amounts of the peptide to be detected using this pull-down and western blot method, even when given chronically. However, this method did reveal biotin-TAT-c29 peptide in brains of mice treated for 6 weeks with 8mg/kg and 5mg/kg. This result indicated biotin-TAT-c29 had the ability to cross the blood brain barrier and reach the brain

.

Finally, we used the 9992 antibody to immunostain brain sections of tissue from control or biotin-TAT-c29 treated animals. Unfortunately, significant staining was seen with this antibody in un-injected animals, most likely due to endogenous p75NTR. p75NTR is expressed in the basal forebrain neurons and their axons which project to nearly the entire brain. It was therefore difficult to develop the DAB immunostaining to optimise detection of the peptide without overstaining the sections for $p75^{NTR}$, and a definitive conclusion could not be made regarding the presence of biotin-TAT-c29 in the brain by this method

While the adult brain expresses p75NTR in the basal forebrain throughout life, the adult spinal cord cells do not express p75NTR post development (Bothwell, 1995). We therefore examined the distribution of biotin-TAT-c29 peptide using the 9992 antibody in sections of spinal cord sections from the injected animals. Spinal cord sections of biotin-TAT-c29 treated mice displayed significantly more immunoreactivity than those from control animals (Fig 4.7)

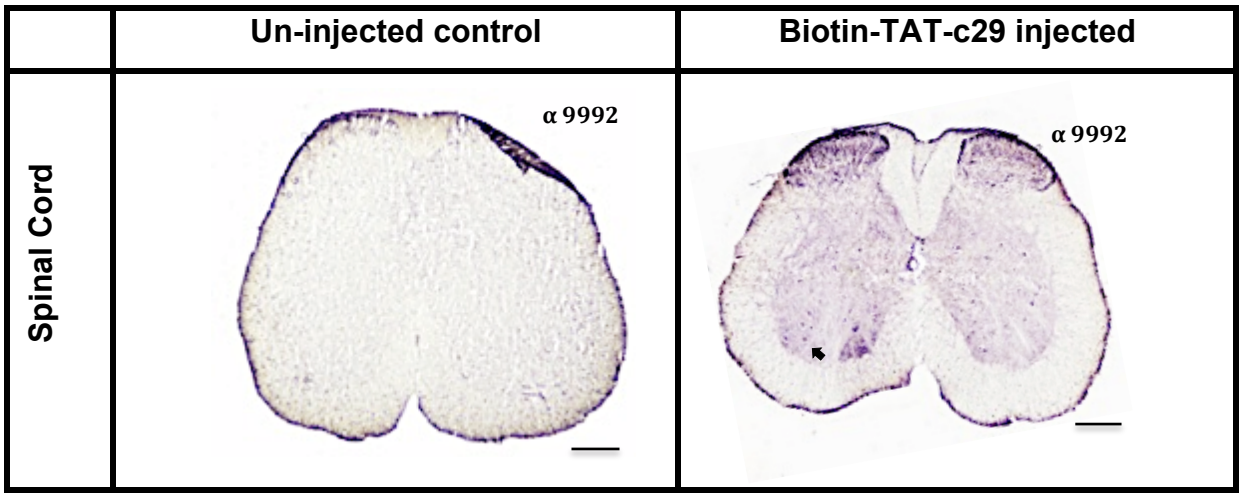

Figure 4.7: Detection of bition-TAT-c29 in the spinal cord using an intracellular p75NTR (9992) antibody
Bright field photomicrographs (10x) of transverse sections through the lumbar spinal cord of control un-injected animal and 8mg/kg biotin-TAT-c29 treated mouse sacrificed 6 weeks after intraperitoneal injections. The sections were immunostained using intracellular p75NTR (9992) antibody developed using DAB. (n=2, Scale bars: 1mm, 10x magnification).

Immuno-positive anti-$p75^{NTR}$ staining in spinal cord sections of biotin-TAT-c29 treated animals was again primarily in the grey matter and also appeared to specifically label motor neurons within the ventral horn (as indicated by the black arrow). At the dorsal horn, immunostaining was also evident in the projections from the dorsal root ganglion in marked contrast in immunostaining in control tissue. This indicated that i.p injection of

biotin-TAT-c29 resulted in delivery of the peptide to cells within the spinal cord and thus potentially throughout the CNS.

Although no method definitively demonstrated biotin-TAT-c29 was delivered within neurons of the brain, together these results make a compelling case the peptide can cross the blood-brain barrier following systemic.

4.2.2. ERK activation – A possible mechanism for c29 action?

One of the proposed mechanisms of biotin-TAT-c29 action is its ability to interact with and enhance Trk mediated survival signalling. We have previously reported the ability of c29 peptide to promote neurite outgrowth through activation of trophic Erk1/2 and AKT signalling cascades mediated by Trk receptor activity (Matusica et al., 2013).

PC12 neuronal cells endogenously express both TrkA and p75NTR receptor and are widely used to study actions of neurotrophins on their receptors. For the purpose of our experiment we assessed the level of phosphorylated ERK1/2, activated by NGF treatment of PC12 cells alone, compared with the level in PC12 cells treated with NGF and biotin-TAT-c29. An increase in 10ng/ml NGF mediated ERK1/2 phosphorylation to a similar extent as that induced by treatment with 10 fold higher NGF concentrations (100ng/ml) was induced by c29 treatment (figure 4.8).

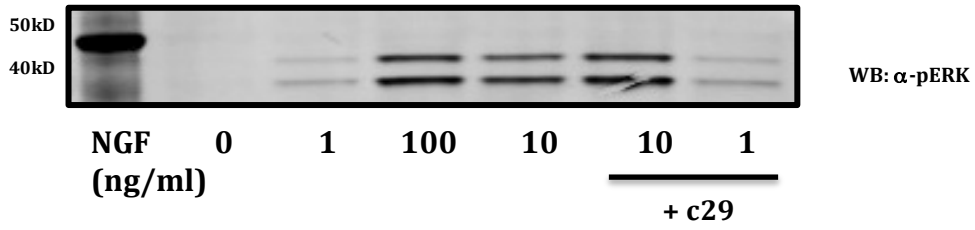

Figure 4.8. – Biotin-TAT-c29 in the presence of limited NGF induces an enhanced ERK response in PC12 cells

Lane 1: ladder, lane 2-4: PC12 cells treated with either 0ng/ml, 1ng/ml or 100ng/ml NGF, lane 5-6: PC12 cells treated with biotin-TAT-c29 at 100uM with either 10ng/ml or 1ng/ml NGF. The western blot was probed with anti-phosphoERK primary antibody. NGF treatment up-regulates the level of pERK in a dose dependent manner. No response was noted in the absence of NGF. In the presence of c29 with 10ng/ml NGF, a response equivalent to 100ng NGF alone could be seen, suggesting that c29 increases the sensitivity of PC12 cells to NGF treatment.

We therefore hypothesised that following delivery to the brain, c29 would potentiate Trk receptor-mediated signalling *in vivo*, resulting in increased (above baseline) ERK1/2 levels

in neurons of the brain and spinal cord. Such a result would provide indirect evidence that biotin-TAT-c29 was entering the neurons within the brain and spinal cord but also provide evidence for c29 mediating trophic effect in those neurons. Mice were injected with 8mg/kg peptide and scarified 7 days later and immunostained for phosphorylated ERK1/2.

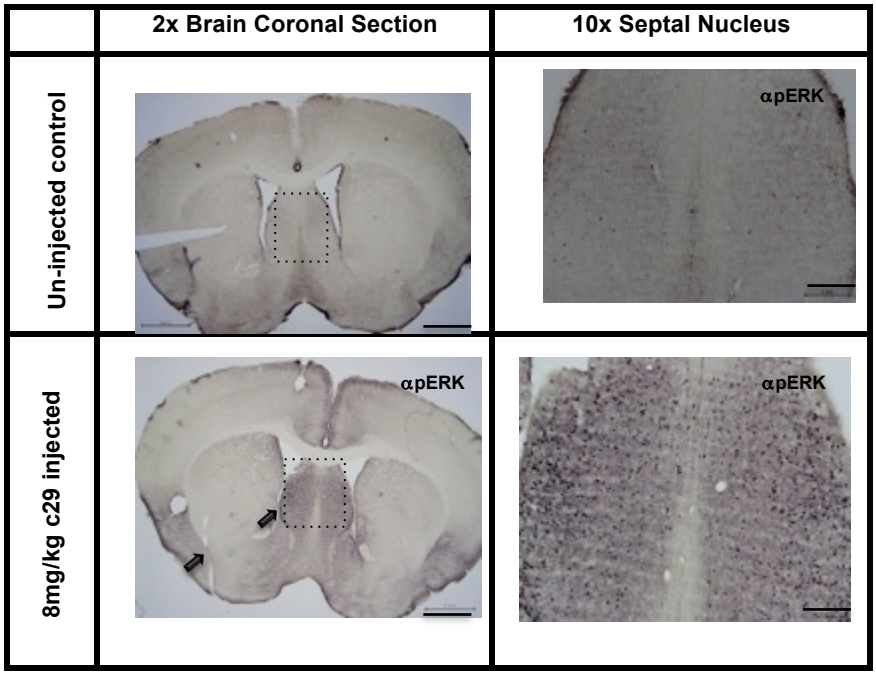

Figure 4.9. - Detection of Erk activation in the brain post c29 peptide injection using a pERK antibody in the brain

Bright field photomicrographs (2x, 10x) of the brain at the level of the basal forebrain were immunostained with anti phosphorylated-ERK (pERK) antibody to allow detection of activated ERK. 10x photomicrograph show activated neurons in the septal nucleus of the basal forebrain specifically (n=3, Scale bars: 1mm).

In biotin-TAT-c29 treated mice, strong immunostaining for phosphorylated Erk1/2-immunopositive cells were observed in the septal and cortical areas, whereas, significantly reduced staining was seen in these areas in the un-injected control (figure 4.9). These areas express the TrkB receptor and BDNF, which is released in a synaptic-activity dependent manner, but essentially constitutively.

The extent of phosphorylated Erk1/2-immunostaining in the spinal cord of mice treated with biotin-TAT-c29 was similarly assessed, revealing enhanced immunostaining in the motor neurons of the ventral horn expressing the TrkB receptor (figure 4.10). Again the immunostaining was primarily within the cell bodies rather than white matter. These results

indicate that not only does TAT-c29 cross the blood brain barrier but that it may mediate enhanced trophic signalling, as occurs *in vitro*.

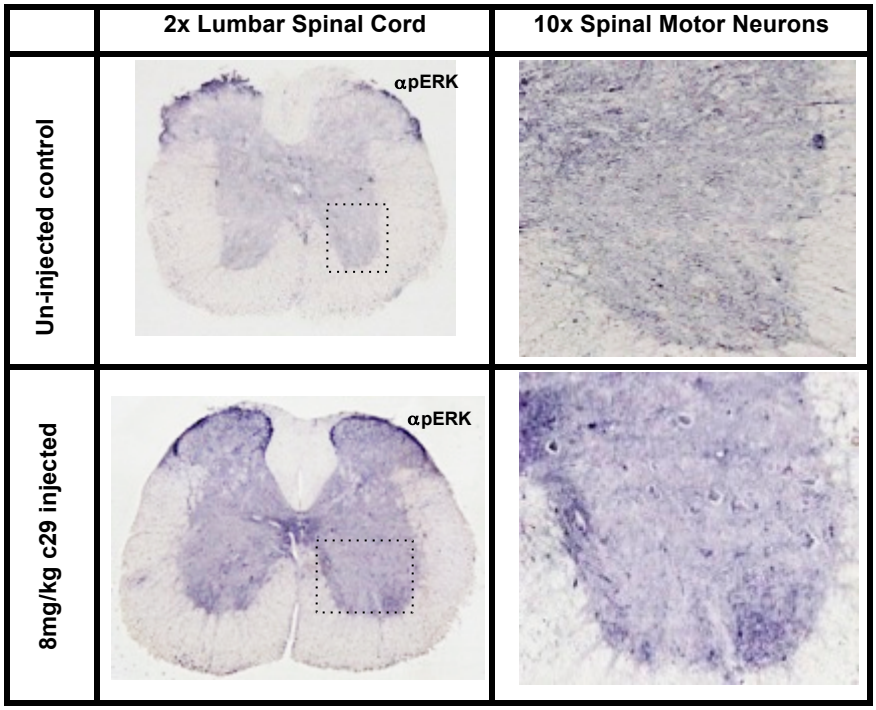

Figure 4.10. – Detection of Erk activation in the brain post c29 peptide injection using a pERK antibody in the spinal cord

Bright field photomicrographs (2x, 10x) of the brain at the level of the lumbar spinal cord were immunostained with anti phosphorylated-ERK (pERK) antibody to allow detection of activated ERK. 10x photomicrograph show activated motor neurons in the ventral horn of the lumbar spinal cord (n=3, Scale bars: 1mm).

4.2.3. Does c29 cause neuro-inflammation?

Systemic delivery of any phamacological compound has the potential to cause side effects. No obvious adverse effects were observed for mice injected with the peptide chronically over 6 weeks, however this does not rule out toxicity as this aspect was not comprehensively studied herein. However, inflammation in the brain may indicate neurotoxicity or an detrimental immunological response caused by the peptide. We therefore measured the number of reactive astrocytes and microglia in the brain as an indicator of neuro-inflammation. We used a GFAP antibody to stain for any change in astrocyte number and morphology that would indicate astrocytic activation.

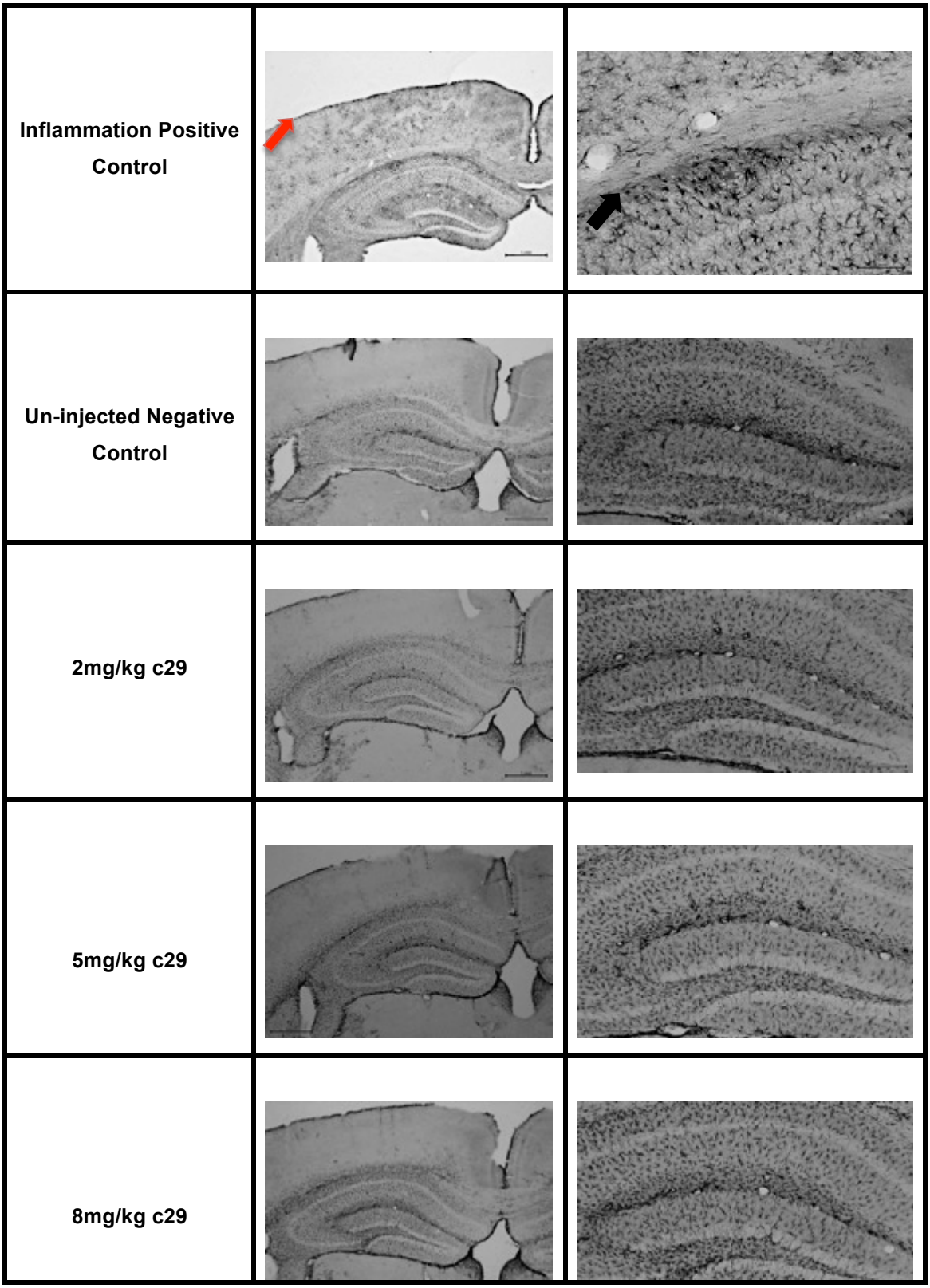

Figure 4.11 – Biotin-TAT-c29 peptide injections do not cause inflammation in the brain

Hippocampal sections of mice injected with either 2mg/kg, 5mg/kg or 8mg/kg of peptide for 6 weeks compared to a negative control (un-injected brain) and a positive control (an aged Alzheimer's disease brain). The staining was performed using a GFAP antibody (n=2, scale bars 1mm, magnification 10x and 20x).

The brain of an aged Alzheimer's disease mouse model (APP/PS1) was used as a positive control for neuroinflammation within in the hippocampus and cortex. In the APP/PS1 mice, but not GFAP–positive astrocytes were present in the cortex (red arrow) but not in the naïve wild-type mice or the biotin-TAT-c29 treated animals (Fig 4.10). In addition, neither naïve nor biotin-TAT-c29 treated animals showed increased activation of reactive astrocytes, indicated by upregulated GFAP intensity and larger irregular processes, in the hippocampus, in contrast to the immunostaining in the hippocampus of APP/PS animals (Fig 4.10). This indicated that biotin-TAT-c29 treatment over 6 weeks does not result in inflammation of the brain.

4.3. Discussion

The main aim of this work was to optimize delivery and detection of biotin-TAT-c29 into the brain and spinal cord of adult mice. Three different methods of biotin-TAT-c29 detection provided results following intraperitoneal injections: i) biotin detection, ii) detection using the 9992 p75NTR antibody and iii) staining for the effects of biotin-TAT-c29, activated ERK, using pERK antibody.

When taken together, the results from the above experiments assessing peptide delivery into the central nervous system indicate that biotin-TAT-c29 can be successfully delivered to brain and spinal cord by intraperitoneal administration. In summary, biotin-TAT-c29 was recovered from brain lysates using pull-downs as biotin-immunopositivity was present in the brain using streptavidin conjugated antibodies (although background staining due to the endogenous biotin was also present as a confound), and while detection of biotin-TAT-c29 in the brain was not possible using a p75NTR specific antibody (9992) due to coincident staining for endogenous p75NTR present in the adult basal forebrain, it was observed in the spinal cord. Furthermore, increased activation of ERK1/2 was observed in both brain and spinal cord following treatment of mice with biotin-TAT-c29. A possible experiment to allow direct detection of biotin-TAT-c29 in the brain using the 9992 antibody is through injection of the peptide into p75NTR-knockout mice, which our lab currently possesses. These findings add to the increasing body of work demonstrating the successful use of TAT-like PTDs to mediate the delivery of peptides to tissues including the CNS *in vivo* following systemic administration (Tao and Johns, 2008, Tao et al., 2008).

This work also provides evidence for one of the possible mechanisms by which biotin-TAT-c29 may act to prevent cell death. According to publications from our lab, c29 either

mediates its actions by enhancing Trk signalling (Matusica et al., 2013) or by acting in a dominant negative manner by blocking the p75NTR receptor (Coulson et al., 2000a). The above results indicate that biotin-TAT-c29 caused increased activation of Erk1/2 signalling in cells of the brain and spinal cord. According to our model, the increased signalling is due to enhanced activation of the Trk receptors in response to endogenous ligands. TrkB is the predominant Trk receptor and is expressed widely throughout most of the neurons of the brain (Yan et al, 1997) and was likely mediating biotin-TAT-c29's effects In the spinal cord however, Erk signalling was not as strong in the TrkB positive motor neurons. Truncated isoforms of TrkB are known to exist in the brain and spinal cord and it is possible that the spinal motor neurons express a truncated isoform of TrkB which could mean that biotin-TAT-c29 was unable to activate Erk to similar level in the spinal cord. It is also possible that endogenous levels of BDNF were not sufficiently present in the otherwise naïve mice to trigger activation of the Trk receptors even with biotin-TAT-c29 being present. Additional experiments in which release of endogenous growth factors are triggered by a relevant stimuli around the time of administration of biotin-TAT-c29 could test a direct correlation between the effects of biotin-TAT-c29, ligand-induced Trk receptor activation and extent of ERK1/2 phosphorylation.

Chapter 5 - The efficacy of c29 in preventing neurodegeneration

5.1. Background

In chapter 3, we established that the MPT-derived neurotrophin-withdrawal model of cholinergic basal forebrain death and the Aβ hippocampal degeneration model were two appropriate models of degeneration which could be used to test the efficacy of the biotin-TAT-c29 peptide to be neuroprotective. In the second model, an increase in Aβ accumulation in the hippocampus is induced by ablating the cholinergic basal forebrain neurons, a finding that has now been replicated by several independent laboratories. We and others have postulated that the induction of Aβ plaques due to loss of cholinergic innervation to the hippocampus causes a reduction in BDNF released by the hippocampus, which in turn promotes cleavage of APP along the amyloidogenic pathway. The increased production of Aβ could in turn promote neuronal toxicity via p75NTR (Coulson et al., 2008, Sotthibundhu et al., 2008, Yang et al., 2008, Knowles et al., 2009).. We therefore asked whether biotin-TAT-c29 can prevent basal forebrain lesion-induced plaque accumulation and toxicity in the APP/PS1 mouse model.

Although we had established the basal forebrain lesion model by infusing p75NTR-SAP in to the ventricles, we decided to lesion the basal forebrain using a direct injection to the septum. Another laboratory member (Zoran Boskovic) in parallel to my work had established the coordinates for the direct septal lesions and this method had proved to minimise the variability of lesion size when the toxin was injected into the ventricle. Secondly, we chose to use osmotic pumps to deliver the biotin-TAT-c29 peptide, instead of the biotin-TAT-c29 bolus delivered by daily intraperitoneal injections.

5.2. Results

5.2.1. Mini-osmotic pump delivery of biotin-TAT-c29

In chapter 4, it was demonstrated that biotin-TAT-c29 could be successfully administered into the mouse central nervous system using intraperitoneal injections. However, the prolonged delivery times and the manual effort of delivery through injections encouraged us to explore mini-osmotic pumps as a delivery method of biotin-TAT-c29 peptide into mice. Using mini-osmotic pumps would allow consistent and timely administration of the peptide for extended periods of time without the manual labour of injections every 24-72 hours.

As a pilot experiment, 7-day mini-osmotic pumps were placed subcutaneously to deliver an 8mg/kg dose. The effects were compared to control (scrambled peptide)-treated animals. The brain was analysed for effect by immunostaining for activated pERK (figure 5.1).S

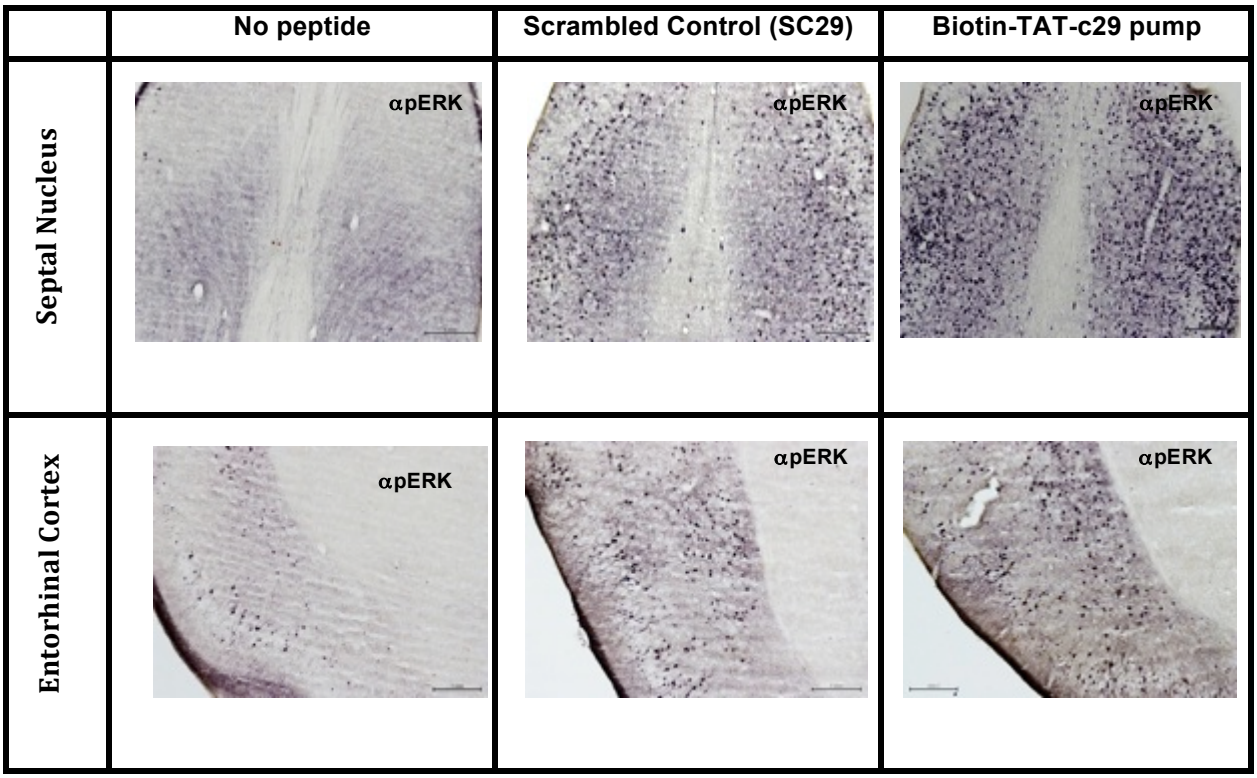

Figure 5.1. – Phosphorylated ERK can be detected in the brain of mice using subcutaneous pump as a delivery method

Bright field photomicrographs (10x) of mice implanted with a 7 day mini-osmotic pump to deliver 8mg/kg of biotin-TAT-c29 peptide were stained using an anti phosphorylated-Erk antibody to detect activated Erk. No peptide control and scrambled biotin-TAT-c29 peptide were used as controls. Activated ERK was noted in two main areas: the septal nucleus of the basal forebrain and the Entorhinal cortex (n=3, Scale bars: 1mm, magnification 10x)

Following 7 days of biotin-TAT-c29 treatment via subcutaneous osmotic pump enhanced Erk1/2 activation was observed in several brain areas. The septal nucleus again displayed the strongest pERK immunostaining compared to levels in naive control mice. Interestingly, the control peptide treatment also raised levels of ERK activation, although to an lesser degree that the activation induced by biotin-TAT-c29 treatment (Fig 5.1). Enhanced Erk1/2 staining due to biotin-TAT-c29 treatment compared to either control was also noted in cortical areas including the Entorhinal cortex (Fig 5.1), an area implicated in

learning and memory, and which is particularly susceptible to degeneration in AD. These results indicated that osmotic pump delivery of biotin-TAT-c29 could elicit a trophic response.

5.2.3. Biotin-TAT-c29 delivery into APP/PS1 mice

At the age of 13-15 weeks, APP/PS1 mice were injected with p75NTR-saporin toxin (or IgG-saporin control toxin) directly into the medial septal area of the basal forebrain to cause a specific cholinergic neuron lesion. During the surgery, mice were also implanted with a subcutaneous 28-day mini-osmotic pump containing either PBS or Biotin-TAT-c29 (10mg/kg). 28-days post surgery, animals were perfused and their brains prepared for histological assessment by immunostaining. ChAT postive neurons in the basal forebrain were counted to determine the lesion size and Aβ plaques were stained with Thiofavin S and the number of plaques per hippocampus were counted (Fig 5.2b). The number of Aβ plaques was not significantly different between treatment groups (Fig 5.2). However this result is confounded by both a mixed gender of animals (Fig 5.2) and lesion sizes that were significantly different between groups (Fig 5.3).

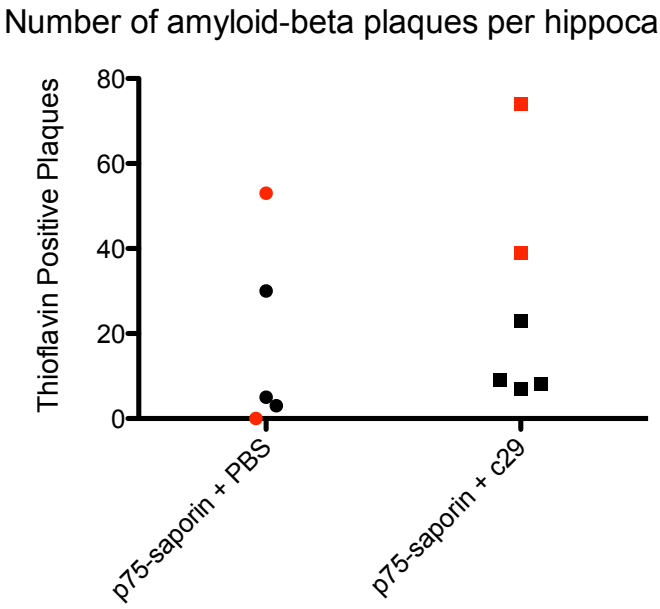

Figure 5.2: No significant difference in the number of Aβ plaques was found between mice treated with PBS and those treated with biotin-TA-c29 peptide

Aβ plaques stained with Thioflavin S were counted in hippocampal sections. The graph represents the total number of Thioflavin S-positive plaques in the entire hippocampus of mice treated with either PBS control (n=5) or biotin-TAT-c29 peptide (n=6). No difference was seen in the number of Aβ plaques of the control versus the c29 treated group. Red dots indicate female mice whereas black squares indicate male mice.

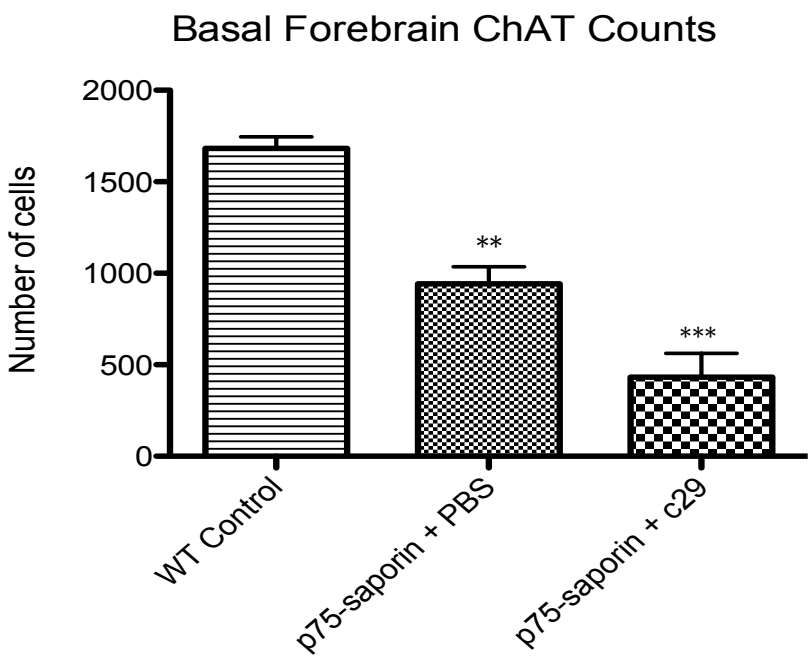

Figure 5.3 - Loss of basal forebrain ChAT positive neurons with p75-saporin toxin

The graph shows the average number of ChAT positive neurons in the basal forebrain region of 13-15weeks old APP/PS1 mice with basal forebrain lesions compared to unnlesioned mice. A decrease in the number of ChAT positive neurons in the basal forebrain of APP/PS1 mice was induced by p75NTR-saporin injections. Mice implanted with a PBS-releasing pump have a 46% reduction in ChAT positive neurons (p=0.0015, n=5) whereas mice treated with biotin-TAT-c29 have a 74% reduction in Chat-positive neurons (p= 0.0002, n=6).

5.3. Discussion

The main aim of this part of my project was to investigate the efficacy of biotin-TAT-c29 in preventing neuronal degeneration in one or more of the mouse models developed in aim 1. Firstly, delivery of the peptide through osmotic pumps was optimized to allow convenient and timely administration of the peptide. Secondly, a new method to directly and specifically lesion the basal forebrain was adopted. Finally, APP/PS1 mice with a cholinergic lesion were treated with biotin-TAT-c29 peptide to rescue Aβ plaque accumulation.

Mini-osmotic pumps have been widely used for the delivery of peptides into the central nervous system (Ittner et al., 2010, Pfluger et al., 2011, Srivareerat et al., 2011). For the purpose of our experiment, subcutaneous mini-osmotic pumps successfully delivered the biotin-TAT-c29 peptide into the brain as detected by enhanced phosphorylation of ERK1/2. The staining was particularly obvious in the septal nucleus and the entorhinal cortex.

There was also a large variability noted in plaque number between groups and between mice. Our study used mixed cohorts of males and females, and according to our Aβ plaque counts, females on average appear to have more plaques (regardless of treatment). Literature suggests that females bear a heavier amyloid beta plaque burden compared to males which could explain our results being skewed due to the gender mixed cohorts (Wang et al., 2003, Yan et al., 2009) . As previously mentioned in chapter 3, APP/PS1 mice have an onset of plaque deposition at 4 months and the purpose of our experiment was to accelerate this plaque production by lesioning the basal forebrain and therefore we decided to use mice as young as 13 weeks. This could have also caused discrepancy in our results as the mice were extremely young and may not have begun accumulating plaques. Inter-mice differences could mean that some mice have a later onset of plaques than the others. For future experiments, the use of mice at 16 weeks would be ideal to allow the onset of Aβ accumulation before accelerating it.
Although this experiment was not particularly encouraging regarding positive benefits of biotin-TAT-c29, a number of changes are proposed to improve the experimental design and thus the ability to draw conclusions regarding the effect of biotin-TAT-c29 treatment in this paradigm. Firstly, same sex (preferably male) mice should be used which are born within one week of each other and used at 16 weeks, to allow the onset of Aβ accumulation before accelerating it.

Secondly, ideally p75NTR-saporin toxin surgery should be performed a week before the mini-osmotic pumps containing the peptide are implanted. Experiments performed by others in the lab have shown that p75NTR-saporin toxin can ablate p75NTR neurons in the basal forebrain as early as 7 days. This would mean that the basal forebrain could be lesioned independently of c29 peptide treatment. Initiating treatment one week after surgery for 28 days would still allow a direct measure of the effect of c29 peptide on Aβ plaque accumulation. Finally, larger cohorts should be used. This would minimise the experimental variation in lesioning size between groups and also enable behavioural experiments such as Morris Water Maze or novel objection recognition to coincidently test hippocampal-dependent cognitive function in addition to measurement of Aβ load and degeneration.

Although this experiment was inconclusive, biotin-TAT-c29 peptide has not only been neuroprotective in *in vitro* experiments performed during my candidature, but others in the

lab have found evidence for its therapeutic effects *in vivo* as well. Systemic treatment of biotin-TAT-c29 was shown to promote motor neuron survival in the SOD1G93A mouse model of motor neuron, mid way through disease progression, with coincident although transient enhanced performance on rotor rod task (manuscript submitted). In addition, intraperitoneal injection biotin-TAT-c29 caused enhanced long-term potentiation (LTP) in the hippocampus. Finally daily i.p injections of biotin-TAT-c29 have enhanced precise spatial memory of 6-8 months old APP/PS1 mice in the Morris water maze.

Concluding Remarks

The overarching aim of this study was to begin to examine the neuroprotective abilities of a novel candidate therapeutic peptide in neurodegenerative mouse models. Previously, this novel peptide (biotin-TAT-c29) had shown to be neuroprotective *in vitro* in: i) conditions of neurotrophin withdrawal and ii) protective against amyloid beta mediated toxicity, both of which are known features of Alzheimer's disease. In order to test the effects of this peptide *in vivo*, models that encompasses a form of neurotrophin-dependent degeneration or Aβ-mediated toxicity were established. The efficacy of this peptide could then be tested *in vivo* in these Alzheimer's disease mouse models. We also provided strong evidence that biotin-TAT-c29 not only crosses the blood brain within 1 hour after systemic administration but can mediate enhanced trophic signalling, enabling biotin-TAT-c29 to be given as a systemic treatment rather than requiring invasive intraventricular infusion, or substantial modification to make it blood-brain permeable. Finally, while the attempt to determine the effect of c29 peptide in the Aβ hippocampal degeneration model was inconclusive, parallel work in our laboratory has provided encouraging evidence that given systemically, c29 is a promising therapeutic peptide. Nonetheless, substantial further work (as indicated under each aim) will be required to conclusively determine whether it has neuroprotective properties in models of neurodegeneration.

Bibliography

Asoh S, Ohsawa I, Mori T, Katsura K, Hiraide T, Katayama Y, Kimura M, Ozaki D, Yamagata K, Ohta S (2002) Protection against ischemic brain injury by protein therapeutics. Proc Natl Acad Sci U S A 99:17107-17112.

Auld DS, Kornecook TJ, Bastianetto S, Quirion R (2002) Alzheimer's disease and the basal forebrain cholinergic system: relations to beta-amyloid peptides, cognition, and treatment strategies. Prog Neurobiol 68:209-245.

Barker PA (2004) p75NTR is positively promiscuous: novel partners and new insights. Neuron 42:529-533.

Bartus RT, Dean RL, 3rd, Beer B, Lippa AS (1982) The cholinergic hypothesis of geriatric memory dysfunction. Science 217:408-414.

Boncristiano S, Calhoun ME, Kelly PH, Pfeifer M, Bondolfi L, Stalder M, Phinney AL, Abramowski D, Sturchler-Pierrat C, Enz A, Sommer B, Staufenbiel M, Jucker M (2002) Cholinergic changes in the APP23 transgenic mouse model of cerebral amyloidosis. J Neurosci 22:3234-3243.

Bothwell M (1995) Functional interactions of neurotrophins and neurotrophin receptors. Annu Rev Neurosci 18:223-253.

Brooks AI, Cory-Slechta DA, Bowers WJ, Murg SL, Federoff HJ (2000a) Enhanced learning in mice parallels vector-mediated nerve growth factor expression in hippocampus. Hum Gene Ther 11:2341-2352.

Brooks AI, Cory-Slechta DA, Federoff HJ (2000b) Gene-experience interaction alters the cholinergic septohippocampal pathway of mice. Proc Natl Acad Sci U S A 97:13378-13383.

Butterfield DA, Howard BJ, Yatin S, Allen KL, Carney JM (1997) Free radical oxidation of brain proteins in accelerated senescence and its modulation by N-tert-butyl-alpha-phenylnitrone. Proc Natl Acad Sci U S A 94:674-678.

Butterfield DA, Poon HF (2005) The senescence-accelerated prone mouse (SAMP8): a model of age-related cognitive decline with relevance to alterations of the gene expression and protein abnormalities in Alzheimer's disease. Exp Gerontol 40:774-783.

Cao G, Pei W, Ge H, Liang Q, Luo Y, Sharp FR, Lu A, Ran R, Graham SH, Chen J (2002) In Vivo Delivery of a Bcl-xL Fusion Protein Containing the TAT Protein Transduction Domain Protects against Ischemic Brain Injury and Neuronal Apoptosis. J Neurosci 22:5423-5431.

Capsoni S, Giannotta S, Cattaneo A (2002) Beta-amyloid plaques in a model for sporadic Alzheimer's disease based on transgenic anti-nerve growth factor antibodies. Mol Cell Neurosci 21:15-28.

Capsoni S, Ugolini G, Comparini A, Ruberti F, Berardi N, Cattaneo A (2000) Alzheimer-like neurodegeneration in aged antinerve growth factor transgenic mice. Proc Natl Acad Sci U S A 97:6826-6831.

Catts VS, Al-Menhali N, Burne TH, Colditz MJ, Coulson EJ (2008) The p75 neurotrophin receptor regulates hippocampal neurogenesis and related behaviours. Eur J Neurosci 28:883-892.

Ceni C, Kommaddi RP, Thomas R, Vereker E, Liu X, McPherson PS, Ritter B, Barker PA (2010) The p75NTR intracellular domain generated by neurotrophin-induced receptor cleavage potentiates Trk signaling. J Cell Sci 123:2299-2307.

Chun W, Johnson GV (2007) The role of tau phosphorylation and cleavage in neuronal cell death. Front Biosci 12:733-756.

Clark SD, Nothacker HP, Wang Z, Saito Y, Leslie FM, Civelli O (2001) The urotensin II receptor is expressed in the cholinergic mesopontine tegmentum of the rat. Brain Res 923:120-127.

Coulson EJ, May LM, Osborne SL, Reid K, Underwood CK, Meunier FA, Bartlett PF, Sah P (2008) p75 neurotrophin receptor mediates neuronal cell death by activating GIRK channels through phosphatidylinositol 4,5-bisphosphate. J Neurosci 28:315-324.

Coulson EJ, May LM, Sykes AM, Hamlin AS (2009) The role of the p75 neurotrophin receptor in cholinergic dysfunction in Alzheimer's disease. Neuroscientist 15:317-323.

Coulson EJ, Reid K, Baca M, Shipham KA, Hulett SM, Kilpatrick TJ, Bartlett PF (2000a) Chopper, a new death domain of the p75 neurotrophin receptor that mediates rapid neuronal cell death. J Biol Chem 275:30537-30545.

Coulson EJ, Reid K, Barrett GL, Bartlett PF (1999) p75 neurotrophin receptor-mediated neuronal death is promoted by Bcl-2 and prevented by Bcl-xL. J Biol Chem 274:16387-16391.

Coulson EJ, Reid K, Murray SS, Cheema SS, Bartlett PF (2000b) Role of neurotrophin receptor p75NTR in mediating neuronal cell death following injury. Clin Exp Pharmacol Physiol 27:537-541.

Coulson EJ, Reid K, Shipham KM, Morley S, Kilpatrick TJ, Bartlett PF (2004) The role of neurotransmission and the Chopper domain in p75 neurotrophin receptor death signaling. Prog Brain Res 146:41-62.

Coyle JT, Price DL, DeLong MR (1983) Alzheimer's disease: a disorder of cortical cholinergic innervation. Science 219:1184-1190.

Davies AM (1991) Nerve growth factor synthesis and nerve growth factor receptor expression in neural development. Int Rev Cytol 128:109-138.

Dechant G, Barde YA (2002) The neurotrophin receptor p75(NTR): novel functions and implications for diseases of the nervous system. Nat Neurosci 5:1131-1136.

Del Valle J, Duran-Vilaregut J, Manich G, Casadesus G, Smith MA, Camins A, Pallas M, Pelegri C, Vilaplana J (2010) Early amyloid accumulation in the hippocampus of SAMP8 mice. J Alzheimers Dis 19:1303-1315.

Duff K, Eckman C, Zehr C, Yu X, Prada CM, Perez-tur J, Hutton M, Buee L, Harigaya Y, Yager D, Morgan D, Gordon MN, Holcomb L, Refolo L, Zenk B, Hardy J, Younkin S (1996) Increased amyloid-beta42(43) in brains of mice expressing mutant presenilin 1. Nature 383:710-713.

Fahnestock M, Michalski B, Xu B, Coughlin MD (2001) The precursor pro-nerve growth factor is the predominant form of nerve growth factor in brain and is increased in Alzheimer's disease. Mol Cell Neurosci 18:210-220.

Flood JF, Morley JE (1993) Age-related changes in footshock avoidance acquisition and retention in senescence accelerated mouse (SAM). Neurobiol Aging 14:153-157.

German DC, Yazdani U, Speciale SG, Pasbakhsh P, Games D, Liang CL (2003) Cholinergic neuropathology in a mouse model of Alzheimer's disease. J Comp Neurol 462:371-381.

Ginsberg SD, Che S, Wuu J, Counts SE, Mufson EJ (2006) Down regulation of trk but not p75NTR gene expression in single cholinergic basal forebrain neurons mark the progression of Alzheimer's disease. J Neurochem 97:475-487.

Glenner GG, Wong CW (1984) Alzheimer's disease and Down's syndrome: sharing of a unique cerebrovascular amyloid fibril protein. Biochem Biophys Res Commun 122:1131-1135.

Gotz J, Eckert A, Matamales M, Ittner LM, Liu X (2011) Modes of Abeta toxicity in Alzheimer's disease. Cell Mol Life Sci 68:3359-3375.

Gu Z, Yu J, Perez-Polo JR (1998) Long term changes in brain cholinergic markers and nerve growth factor levels after partial immunolesion. Brain Res 801:190-197.

Gupta B, Levchenko TS, Torchilin VP (2005) Intracellular delivery of large molecules and small particles by cell-penetrating proteins and peptides. Adv Drug Deliv Rev 57:637-651.

Gutierrez H, Miranda MI, Bermudez-Rattoni F (1997) Learning impairment and cholinergic deafferentation after cortical nerve growth factor deprivation. J Neurosci 17:3796-3803.

Hardy J, Duff K, Hardy KG, Perez-Tur J, Hutton M (1998) Genetic dissection of Alzheimer's disease and related dementias: amyloid and its relationship to tau. Nat Neurosci 1:355-358.

Hardy J, Selkoe DJ (2002) The amyloid hypothesis of Alzheimer's disease: progress and problems on the road to therapeutics. Science 297:353-356.

Härtig W, Saul A, Kacza J, Grosche J, Goldhammer S, Michalski D, Wirths O (2013) Immunolesion-induced loss of cholinergic projection neurons promotes β-amyloidosis and tau hyperphosphorylation in the hippocampus of triple-transgenic mice. Neuropathol Appl Neurobiol n/a-n/a.

Hempstead BL, Martin-Zanca D, Kaplan DR, Parada LF, Chao MV (1991) High-affinity NGF binding requires coexpression of the trk proto-oncogene and the low-affinity NGF receptor. Nature 350:678-683.

Hennigan A, O'Callaghan RM, Kelly AM (2007) Neurotrophins and their receptors: roles in plasticity, neurodegeneration and neuroprotection. Biochem Soc Trans 35:424-427.

Hernandez CM, Kayed R, Zheng H, Sweatt JD, Dineley KT (2010) Loss of alpha7 nicotinic receptors enhances beta-amyloid oligomer accumulation, exacerbating early-stage cognitive decline and septohippocampal pathology in a mouse model of Alzheimer's disease. J Neurosci 30:2442-2453.

Holcomb LA, Gordon MN, Jantzen P, Hsiao K, Duff K, Morgan D (1999) Behavioral changes in transgenic mice expressing both amyloid precursor protein and presenilin-1 mutations: lack of association with amyloid deposits. Behav Genet 29:177-185.

Holtzman DM, Morris JC, Goate AM (2011) Alzheimer's disease: the challenge of the second century. Sci Transl Med 3:77sr71.

Huber LJ, Chao MV (1995) Mesenchymal and neuronal cell expression of the p75 neurotrophin receptor gene occur by different mechanisms. Dev Biol 167:227-238.

Huitron-Resendiz S, Kristensen MP, Sanchez-Alavez M, Clark SD, Grupke SL, Tyler C, Suzuki C, Nothacker HP, Civelli O, Criado JR, Henriksen SJ, Leonard CS, de Lecea L (2005) Urotensin II modulates rapid eye movement sleep through activation of brainstem cholinergic neurons. J Neurosci 25:5465-5474.

Iqbal K, Alonso Adel C, Chen S, Chohan MO, El-Akkad E, Gong CX, Khatoon S, Li B, Liu F, Rahman A, Tanimukai H, Grundke-Iqbal I (2005) Tau pathology in Alzheimer disease and other tauopathies. Biochim Biophys Acta 1739:198-210.

Ittner LM, Gotz J (2011) Amyloid-beta and tau--a toxic pas de deux in Alzheimer's disease. Nat Rev Neurosci 12:65-72.

Ittner LM, Ke YD, Delerue F, Bi M, Gladbach A, van Eersel J, Wolfing H, Chieng BC, Christie MJ, Napier IA, Eckert A, Staufenbiel M, Hardeman E, Gotz J (2010) Dendritic function of tau mediates amyloid-beta toxicity in Alzheimer's disease mouse models. Cell 142:387-397.

Jankowsky JL, Fadale DJ, Anderson J, Xu GM, Gonzales V, Jenkins NA, Copeland NG, Lee MK, Younkin LH, Wagner SL, Younkin SG, Borchelt DR (2004) Mutant presenilins specifically elevate the levels of the 42 residue beta-amyloid peptide in vivo: evidence for augmentation of a 42-specific gamma secretase. Hum Mol Genet 13:159-170.

Jegou S, Cartier D, Dubessy C, Gonzalez BJ, Chatenet D, Tostivint H, Scalbert E, LePrince J, Vaudry H, Lihrmann I (2006) Localization of the urotensin II receptor in the rat central nervous system. J Comp Neurol 495:21-36.

Jung KM, Tan S, Landman N, Petrova K, Murray S, Lewis R, Kim PK, Kim DS, Ryu SH, Chao MV, Kim TW (2003) Regulated intramembrane proteolysis of the p75 neurotrophin receptor modulates its association with the TrkA receptor. J Biol Chem 278:42161-42169.

Kanning KC, Hudson M, Amieux PS, Wiley JC, Bothwell M, Schecterson LC (2003) Proteolytic processing of the p75 neurotrophin receptor and two homologs generates C-terminal fragments with signaling capability. J Neurosci 23:5425-5436.

Knowles JK, Rajadas J, Nguyen TV, Yang T, LeMieux MC, Vander Griend L, Ishikawa C, Massa SM, Wyss-Coray T, Longo FM (2009) The p75 neurotrophin receptor promotes amyloid-beta(1-42)-induced neuritic dystrophy in vitro and in vivo. J Neurosci 29:10627-10637.

Kommaddi RP, Thomas R, Ceni C, Daigneault K, Barker PA (2011) Trk-dependent ADAM17 activation facilitates neurotrophin survival signaling. FASEB journal : official publication of the Federation of American Societies for Experimental Biology 25:2061-2070.

Kumar VB, Farr SA, Flood JF, Kamlesh V, Franko M, Banks WA, Morley JE (2000) Site-directed antisense oligonucleotide decreases the expression of amyloid precursor protein and reverses deficits in learning and memory in aged SAMP8 mice. Peptides 21:1769-1775.

Laursen B, M√∏rk A, Plath N, Kristiansen U, Bastlund JF (2013) Cholinergic degeneration is associated with increased plaque deposition and cognitive impairment in APPswe/PS1dE9 mice. Behav Brain Res 240:146-152.

Lee R, Kermani P, Teng KK, Hempstead BL (2001a) Regulation of cell survival by secreted proneurotrophins. Science 294:1945-1948.

Lee VM, Goedert M, Trojanowski JQ (2001b) Neurodegenerative tauopathies. Annu Rev Neurosci 24:1121-1159.

Lowry KS, Murray SS, Coulson EJ, Epa R, Bartlett PF, Barrett G, Cheema SS (2001) Systemic administration of antisense p75(NTR) oligodeoxynucleotides rescues axotomised spinal motor neurons. J Neurosci Res 64:11-17.

Manich G, Mercader C, del Valle J, Duran-Vilaregut J, Camins A, Pallas M, Vilaplana J, Pelegri C (2011) Characterization of amyloid-beta granules in the hippocampus of SAMP8 mice. J Alzheimers Dis 25:535-546.

Masters CL, Simms G, Weinman NA, Multhaup G, McDonald BL, Beyreuther K (1985) Amyloid plaque core protein in Alzheimer disease and Down syndrome. Proc Natl Acad Sci U S A 82:4245-4249.

Matsui N, Takahashi K, Takeichi M, Kuroshita T, Noguchi K, Yamazaki K, Tagashira H, Tsutsui K, Okada H, Kido Y, Yasui Y, Fukuishi N, Fukuyama Y, Akagi M (2009) Magnolol and honokiol prevent learning and memory impairment and cholinergic deficit in SAMP8 mice. Brain Res 1305:108-117.

Matusica D, Skeldal S, Sykes AM, Palstra N, Sharma A, Coulson EJ (2013) An Intracellular Domain Fragment of the p75 Neurotrophin Receptor (p75NTR) Enhances Tropomyosin Receptor Kinase A (TrkA) Receptor Function. J Biol Chem 288:11144-11154.

McKay BE, Molineux ML, Turner RW (2004) Biotin is endogenously expressed in select regions of the rat central nervous system. J Comp Neurol 473:86-96.

McKay BE, Molineux ML, Turner RW (2008) Endogenous biotin in rat brain: implications for false-positive results with avidin-biotin and streptavidin-biotin techniques. Methods Mol Biol 418:111-128.

Miyamoto M (1997) Characteristics of age-related behavioral changes in senescence-accelerated mouse SAMP8 and SAMP10. Exp Gerontol 32:139-148.

Mudher A, Lovestone S (2002) Alzheimer's disease-do tauists and baptists finally shake hands? Trends Neurosci 25:22-26.

Mufson EJ, Brashers-Krug T, Kordower JH (1992) p75 nerve growth factor receptor immunoreactivity in the human brainstem and spinal cord. Brain Res 589:115-123.

Mufson EJ, Lavine N, Jaffar S, Kordower JH, Quirion R, Saragovi HU (1997) Reduction in p140-TrkA receptor protein within the nucleus basalis and cortex in Alzheimer's disease. Exp Neurol 146:91-103.

Nagappan G, Lu B (2005) Activity-dependent modulation of the BDNF receptor TrkB: mechanisms and implications. Trends Neurosci 28:464-471.

Naumann T, Casademunt E, Hollerbach E, Hofmann J, Dechant G, Frotscher M, Barde YA (2002) Complete deletion of the neurotrophin receptor p75NTR leads to long-lasting increases in the number of basal forebrain cholinergic neurons. J Neurosci 22:2409-2418.

Oddo S, Caccamo A, Kitazawa M, Tseng BP, LaFerla FM (2003) Amyloid deposition precedes tangle formation in a triple transgenic model of Alzheimer's disease. Neurobiol Aging 24:1063-1070.

Perez M, Ribe E, Rubio A, Lim F, Moran MA, Ramos PG, Ferrer I, Isla MT, Avila J (2005) Characterization of a double (amyloid precursor protein-tau) transgenic: tau phosphorylation and aggregation. Neuroscience 130:339-347.

Perez SE, Dar S, Ikonomovic MD, DeKosky ST, Mufson EJ (2007) Cholinergic forebrain degeneration in the APPswe/PS1DeltaE9 transgenic mouse. Neurobiol Dis 28:3-15.

Pfluger PT, Castaneda TR, Heppner KM, Strassburg S, Kruthaupt T, Chaudhary N, Halem H, Culler MD, Datta R, Burget L, Tschop MH, Nogueiras R, Perez-Tilve D (2011) Ghrelin, peptide YY and their hypothalamic targets differentially regulate spontaneous physical activity. Physiol Behav 105:52-61.

Poon HF, Joshi G, Sultana R, Farr SA, Banks WA, Morley JE, Calabrese V, Butterfield DA (2004) Antisense directed at the Abeta region of APP decreases brain oxidative markers in aged senescence accelerated mice. Brain Res 1018:86-96.

Prakash N, Cohen-Cory S, Penschuck S, Frostig RD (2004) Basal forebrain cholinergic system is involved in rapid nerve growth factor (NGF)-induced plasticity in the barrel cortex of adult rats. J Neurophysiol 91:424-437.

Ramos OV, Torterolo P, Lim V, Chase MH, Sampogna S, Yamuy J (2011) The role of mesopontine NGF in sleep and wakefulness. Brain Res 1413:9-23.

Ramos-Rodriguez JJ, Pacheco-Herrero M, Thyssen D, Murillo-Carretero MI, Berrocoso E, Spires-Jones TL, Bacskai BJ, Garcia-Alloza M (2013) Rapid Œ≤-Amyloid Deposition and Cognitive Impairment After Cholinergic Denervation in APP/PS1 Mice. Journal of

Neuropathology & Experimental Neurology 72:272-285 210.1097/NEN.1090b1013e318288a318288dd.

Sarter M, Bruno JP (2004) Developmental origins of the age-related decline in cortical cholinergic function and associated cognitive abilities. Neurobiol Aging 25:1127-1139.

Schwarze SR, Ho A, Vocero-Akbani A, Dowdy SF (1999) In vivo protein transduction: delivery of a biologically active protein into the mouse. Science 285:1569-1572.

Selkoe DJ (1989) Biochemistry of altered brain proteins in Alzheimer's disease. Annu Rev Neurosci 12:463-490.

Skeldal S, Matusica D, Nykjaer A, Coulson EJ (2011) Proteolytic processing of the p75 neurotrophin receptor: A prerequisite for signalling?: Neuronal life, growth and death signalling are crucially regulated by intra-membrane proteolysis and trafficking of p75(NTR). Bioessays 33:614-625.

Sotthibundhu A, Sykes AM, Fox B, Underwood CK, Thangnipon W, Coulson EJ (2008) Beta-amyloid(1-42) induces neuronal death through the p75 neurotrophin receptor. J Neurosci 28:3941-3946.

Srivareerat M, Tran TT, Salim S, Aleisa AM, Alkadhi KA (2011) Chronic nicotine restores normal Abeta levels and prevents short-term memory and E-LTP impairment in Abeta rat model of Alzheimer's disease. Neurobiol Aging 32:834-844.

Strong R, Reddy V, Morley JE (2003) Cholinergic deficits in the septal-hippocampal pathway of the SAM-P/8 senescence accelerated mouse. Brain Res 966:150-156.

Sturchler-Pierrat C, Abramowski D, Duke M, Wiederhold KH, Mistl C, Rothacher S, Ledermann B, Burki K, Frey P, Paganetti PA, Waridel C, Calhoun ME, Jucker M, Probst A, Staufenbiel M, Sommer B (1997) Two amyloid precursor protein transgenic mouse models with Alzheimer disease-like pathology. Proc Natl Acad Sci U S A 94:13287-13292.

Takeda T, Hosokawa M, Takeshita S, Irino M, Higuchi K, Matsushita T, Tomita Y, Yasuhira K, Hamamoto H, Shimizu K, Ishii M, Yamamuro T (1981) A new murine model of accelerated senescence. Mech Ageing Dev 17:183-194.

Tanzi RE (2005) The synaptic Abeta hypothesis of Alzheimer disease. Nat Neurosci 8:977-979.

Tanzi RE, Bertram L (2005) Twenty years of the Alzheimer's disease amyloid hypothesis: a genetic perspective. Cell 120:545-555.

Tao F, Johns RA (2008) Effect of disrupting N-methyl-d-aspartate receptor-postsynaptic density protein-95 interactions on the threshold for halothane anesthesia in mice. Anesthesiology 108:882-887.

Tao F, Su Q, Johns RA (2008) Cell-permeable peptide Tat-PSD-95 PDZ2 inhibits chronic inflammatory pain behaviors in mice. Molecular therapy : the journal of the American Society of Gene Therapy 16:1776-1782.

Terry AV, Jr., Buccafusco JJ (2003) The cholinergic hypothesis of age and Alzheimer's disease-related cognitive deficits: recent challenges and their implications for novel drug development. J Pharmacol Exp Ther 306:821-827.

Underwood CK, Coulson EJ (2008) The p75 neurotrophin receptor. Int J Biochem Cell Biol 40:1664-1668.

Underwood CK, Reid K, May LM, Bartlett PF, Coulson EJ (2008) Palmitoylation of the C-terminal fragment of p75(NTR) regulates death signaling and is required for subsequent cleavage by gamma-secretase. Mol Cell Neurosci 37:346-358.

Wang J, Tanila H, Puolivali J, Kadish I, van Groen T (2003) Gender differences in the amount and deposition of amyloidbeta in APPswe and PS1 double transgenic mice. Neurobiol Dis 14:318-327.

Wang YJ, Wang X, Lu JJ, Li QX, Gao CY, Liu XH, Sun Y, Yang M, Lim Y, Evin G, Zhong JH, Masters C, Zhou XF (2011) p75NTR regulates Abeta deposition by increasing Abeta production but inhibiting Abeta aggregation with its extracellular domain. J Neurosci 31:2292-2304.

Whitehouse PJ (1991a) Pathology in the cholinergic basal forebrain: implications for treatment. Adv Exp Med Biol 295:447-452.

Whitehouse PJ (1991b) Treatment of Alzheimer disease. Alzheimer Dis Assoc Disord 5 Suppl 1:S32-36.

Woolf NJ (1991) Cholinergic systems in mammalian brain and spinal cord. Prog Neurobiol 37:475-524.

Woolf NJ, Butcher LL (1986) Cholinergic systems in the rat brain: III. Projections from the pontomesencephalic tegmentum to the thalamus, tectum, basal ganglia, and basal forebrain. Brain Res Bull 16:603-637.

Woolf NJ, Harrison JB, Buchwald JS (1990) Cholinergic neurons of the feline pontomesencephalon. II. Ascending anatomical projections. Brain Res 520:55-72.

Woolf NJ, Hernit MC, Butcher LL (1986) Cholinergic and non-cholinergic projections from the rat basal forebrain revealed by combined choline acetyltransferase and Phaseolus vulgaris leucoagglutinin immunohistochemistry. Neurosci Lett 66:281-286.

Yaar M, Zhai S, Pilch PF, Doyle SM, Eisenhauer PB, Fine RE, Gilchrest BA (1997) Binding of beta-amyloid to the p75 neurotrophin receptor induces apoptosis. A possible mechanism for Alzheimer's disease. J Clin Invest 100:2333-2340.

Yan P, Bero AW, Cirrito JR, Xiao Q, Hu X, Wang Y, Gonzales E, Holtzman DM, Lee JM (2009) Characterizing the appearance and growth of amyloid plaques in APP/PS1 mice. J Neurosci 29:10706-10714.

Yang T, Knowles JK, Lu Q, Zhang H, Arancio O, Moore LA, Chang T, Wang Q, Andreasson K, Rajadas J, Fuller GG, Xie Y, Massa SM, Longo FM (2008) Small molecule, non-peptide p75 ligands inhibit Abeta-induced neurodegeneration and synaptic impairment. PLoS One 3:e3604.